Understanding the crustal architecture beneath the Bangui magnetic anomaly and its interactions with central African tectonic megastructures based gravity and magnetic analysis

Cyrille Donald Njiteu Tchoukeu, Yvette Poudjom Djomani, Kevin Mickus, Sonia Rousse, Mohamed Sobh, Charles Basseka, Jacques Etame

Understanding the Crustal Architecture Beneath the Bangui Magnetic Anomaly and Its Interactions With Central African Tectonic Megastructures Based Gravity and Magnetic Analysis

Cyrille Donald Njiteu Tchoukeu (cyrillenjiteu@gmail.com)
Universite de Douala Faculte des Sciences https://orcid.org/0000-0003-2549-4804

Yvette Poudjom Djomani
Geoscience Australia

Kevin Mickus
Missouri State University

Sonia Rousse
Geoscience Environment Toulouse: Geosciences Environnement Toulouse

Mohamed Sobh
Leibniz Institute for Applied Geophysics: Leibniz-Institut fur Angewandte Geophysik

Charles Basseka
University of Douala Faculty of Sciences: Universite de Douala Faculte des Sciences

Jacques Etame
University of Douala Faculty of Sciences: Universite de Douala Faculte des Sciences

Research Article

Keywords: magnetic anomalies, gravity and magnetic modelling, Proterozoic and Archean Tectonic, Bangui magnetic anomaly, Central Africa

Posted Date: June 26th, 2023

DOI: https://doi.org/10.21203/rs.3.rs-2995552/v1

Abstract

The Bangui magnetic anomaly (BMA) in Central Africa is one of the largest continental magnetic anomalies on Earth in terms of amplitude and lateral size. Determining the sources of the BMA can lead to an increased understanding of the crustal dynamic in the Central African sub-region and the African continent as a whole. Magnetic and gravity analysis-based derivative, two-dimensional forward modelling and a Curie isothermal depth, showed that (a) the bottoms of the magnetic sources were between 15 and 35 km; (b) the BMA is a coalescence of several anomalies that trend E-W and roughly NE-SW. These directions coincide with regional Pan African-aged shear zones along the Central African orogenic belt and to thrust sheets at the northern edge of the Congo Craton. The depth of magnetization does not exceed 35 km with the amplitude of magnetization becoming smaller in the Central African Republic. The potential magnetic susceptibility sources have an average density of 2850 kg/m3 and magnetic susceptibilities between 0.06 and 0.25 SI. The BMA is interpreted to be a combination of middle and lower crustal bodies that are not continuous and consist of magnetic mineral rich granulites and banded iron formations. The gravity and magnetic modelling indicate that the entire crust was involved in the Pan African collisional event similar to what is seen in the Mozambique belt in East Africa. Combined with geological and geochemical studies, the models add evidence that one or two subduction zones were involved in accreting terranes on the northern edge of the Congo Craton. The tectonic accretions caused a crustal remobilization along major shear zones that has locally contributed to a probable circulation of fluids enriched in ferromagnesian minerals during late Neoproterozoic magmatism that created the BMA sources.

Highlights

- Magnetic susceptibility sources of the Bangui Magnetic anomaly were imaged using 2D interactive models and were found to be up to 35 km in depth.
- The sources of the BMA are lower and middle crustal banded iron formations and mafic-rich granulites that are part of the Central African Orogenic Belt at the northern edge of the Congo Craton.
- Integrated with gravity data modelling, the sources of the BMA must be related to tectonic processes
- The depth and extent of the magnetic susceptibility sources suggest that the Central African Orogenic Belt was formed during subduction zone processes between the Saharan Metacraton and the Congo Craton during the latest stages of the Pan African orogeny

1. Introduction

The BMA, one of the most important terrestrial magnetic anomalies within Africa (Fig. 1), has been intensively studied (Godivier and Ledonche, 1962; Benkova et al., 1973; Godivier, 1980; Maus et al., 2009; Vervelidou and Thebault, 2015; Meyer et al., 2017) which has produced numerous and sometimes controversial discussions about its origin ranging from geological to meteoritic models (Marsh, 1977; Regan and Marsh, 1982; Girdler et al., 1992; Ravat, 1989; Ravat et al., 2002; Hemant and Maus, 2005;

Klokocnik et al., 2010; Ouabego et al., 2013; Haggerty, 2014; Ki Kis et al., 2021). These studies have used a variety of methods ranging from derivative analyses to forward modeling to aid in interpreting the BMA (Regan and Marsh, 1982; Marsh, 1977; Njiteu et al., 2021a). Despite of all the above studies, there is still a fundamental question about the sources of the anomaly including its geometry, the lateral and vertical extensions, and its petrophysical characteristics. The knowledge of the sources requires the consideration of several structural parameters, including the crustal magnetic susceptibility architecture (Dorbath et al., 1981; Dorbath et al., 1985; Njiteu et al., 2021b) and the mechanical behaviour of the lithosphere (Njiteu et al., 2021b). The BMA has been linked to the formation of the Congo Craton (Dorbath et al., 1985; Njiteu et al., 2021b) but lies within the Central African Orogenic Belt (CAOB) that marks a Neoproterozoic suture zone between the Congo Craton to the south and the Saharan Metacraton to the north (Figs. 2A; C). This region has two different complexly formed lithospheres where their deep structures are poorly known due to the lack of deep geophysical studies. Widely spaced broadband seismic stations have indicated that the crust is thinner beneath the CAOB and considerably thicker beneath both the Saharan Metacraton and Congo Craton (Sobh et al., 2020; Njiteu et al., 2021b).

Besides broadband seismic models, the northern edge of the Congo Craton is associated with a large positive E-W trending gravity anomaly (Boukeke, 1994; Ngalamo et al., 2017) which overlaps with the BMA (Njiteu et al., 2021a; Njiteu et al., 2021b). Thus, the overlap of large-scale geophysical signatures at the northern edge of the Congo Craton can aid in explaining the deep structure of the region using the satellite based EMAG2-v3 model (Fig. 1a) and ground gravity data. Previous gravity modelling in the region of the BMA (Njiteu et al., 2021a; b) indicated that there is a spatial relationship in Cameroon between a portion of the BMA and a gravity maximum marking the northern boundary of the Congo Craton. Gravity and magnetic data will be analysed to determine the nature and extent of the magnetic susceptibility sources of the BMA from Cameroon to the Central African Republic. The analysis will include the construction of a series of derivative maps and by constructing nine forward models across the BMA. Additionally, to aid in constraining the source depths including Curie isothermal depths, a power spectrum analysis will be performed. The modelling methods will allow us to address: (1) the unknown nature of the deep sources associated with the BMA and (2) the nature of the sources associated with the gravity maximum at the northern edge of the Congo Craton. These modelling methods in conjunction with available geological constraints will aid in determining the depth and geometry of magnetic susceptibility and density sources within and surrounding the CAOB. These sources will then be interpreted in order to determine the source of the BMA and its relation to the tectonic evolution of the region.

2. Tectonic and geological setting of the BMA

The BMA is located at the intersection of the CAOB and the northern edge of the Congo Craton (Fig. 2C). The CAOB extends for over 4000 km from Cameroon to Sudan and has been associated with the Pernambuco Fault in Brazil (Nzenti, 1988). The CAOB is considered to have formed during the collision between the Congo Craton and the Saharan Metacraton during the Pan-African Orogeny (Toteu et al., 2006). At the northern edge of the Congo Craton, the CAOB is a multiple collisional belt that contains

lithologies which reflect regional extension, intense migmatization, high-pressure granulite metamorphism and contains major shear zones including the Central Cameroon Shear Zone (CCSZ), the Sanaga Shear Zone (SSZ), the Tchollire-Banyo Shear zone (TBSZ) and its extension to the Chad (Braitenberg et al., 2011; Toteu et al., 2022; Nzenti, 1988; Toteu et al., 2004; Toteu et al., 2006). The CAOB is marked in the Mesozoic by the development of Cretaceous basins (Doba-Dosseo-Salamat, Fairhead and Okereke, 1987; Genik, 1993; Guiraud and Binks, 1992; Eyike and Ebbing, 2015; Braitenberg, 2015; Maddaloni et al., 2021) due to the reactivation of the shear zones. In Cameroon, the BMA straddles the Yaounde Group and the Congo Craton (Fig. 2C). The Yaounde Group consists of a thrust sheet which borders the Congo craton to the south and contains micaschists, chlorite-schists, amphibolites, paragneiss, orthogneiss, quartzites (Toteu et al., 2022; Owona et al., 2012; Owona et al., 2013), and also pre-syn-tectonic massifs consisting of mafic rocks or rocks of intermediate composition, ultramafic rocks that contain serpentinites. The southern part of the Yaounde Group lies directly in contact with the Congo Craton and is represented by the Mbalmayo schists. The petrological and chemical characteristics of this zone are those of a detrital and argilo-carbonate sedimentary rocks deposited in a platform environment and metamorphosed under green-schist facies conditions (Feybesse et al., 1998; Owona, 2008; Owona et al., 2012).

In the Central African Republic, the CAOB (Fig. 2C) consists of an Archean and Paleo-Proterozoic basement overlain by Neo-Proterozoic meta-sedimentary units. The Archean basement consists of a 2900 Ma high-grade basic metamorphic complex of a variety of lithologies (Lavreau, 1982) including charnockites and gneisses which are characteristic of a pre-Pan-African collision zone that was reactivated during the Pan-African orogeny. The greenstone belts lithologies consist of komatiites, tholeiitic basalts, andesites, itabirites, grauwackes and rhyodacitic tuffs with Archean granitoids (Poidevin et al., 1981; Dostal et al., 1985; Poidevin, 1991). The central part of the Central African Republic contains an Archean and Paleo-Proterozoic complex which constitutes a basement on which lie Pan-African granulites and gneisses (Pin and Poidevin, 1987; Lavreau et al., 1990). The granulites are well exposed in the western and central areas of the Central African Republic; these granulites have been correlated with those of the Ntem Complex in southern Cameroon (Pin and Poidevin, 1987). The high concentration of iron oxides in these granulites indicates that they were derived from a mafic parental magma (Clark, 1999). Pin and Poidevin (1987) showed that the lower crust would have a more mafic composition than at the base of the surface rocks with the emplacement of mafic basalts in the lower crust during Pan-African orogeny being more possible solution. Additionally, these granulites would be the only ones that are stable at depths of nearly 50 km under conditions of high pressure and temperature (Boukeke, 1994).

The northern edge of the Congo Craton in Cameroon, marked by the Yaounde thrust sheet and its extension in Central African Republic (Fig. 2C) and the CAOB, is the location of numerous thermo-tectonic and seismological interactions (Nedelec et al., 1986; Feybesse et al., 1998; Toteu et al., 2004; Penaye et al., 2004; Lerouge et al., 2006). Geological studies have estimated that the northern limit of the Congo Craton to be at the contact zone with the Yaounde Group (Shang et al., 2004; Toteu et al., 2004; Owona, 2008), where the contact has been interpreted to have been caused by the Pan-African orogeny which

formed thrust sheets between 2°N and 3°N (Figs. 2B-C). The Pan-African orogeny along the northern edge of the Congo Craton has been interpreted to have involved two subduction zones that accreted at least two terrains between the Congo Craton and Saharan Metacraton between 750 and 550 Ma (Toteu et al., 2022). The youngest tectonic events (620 – 550 Ma) involved the creation of suture zones (including the CAOB) and magmatism along the northern Congo Craton (Toteu et al., 2022). Gravity studies (Poudjom, 1993; Boukeke et al., 1994; Tadjou et al., 2009; Ngalamo et al., 2018; Njiteu et al., 2021b) have shown that the northern edge of the Congo Craton is defined by a large amplitude gradient, oriented E-W at roughly 4°N of latitude. Modelling of a gravity anomaly parallel to 4°N gravity indicated northward extension at depth of the Congo Craton structures (Boukeke, 1994; Tadjou et al., 2009). Njiteu et al. (2021a; b), while establishing a spatial relationship between the lower lobe of the Bangui magnetic anomaly and the large E-W trending gravity anomaly previously defined at the northern edge of the Congo craton in Cameroon. This interpretation raises two issues: (1) the unknown nature of the deep sources associated with the BMA and consequently (2) the nature of the sources associated with the positive gravity anomaly at the northern edge of the Congo Craton.

3. Significance of the current study

Knowledge of the sources and origin of the BMA is important both in understanding the internal dynamic processes within Cameroon and Central African Republic, and for estimating the structural parameters that define the lithosphere beneath the anomaly. Ki Kis et al. (2021) inverted SWARM satellite magnetic data to show the difficulty in making only one interpretation for the origin of the BMA. Other gravity and magnetic investigations (Regan and Marsh, 1982; Ravat, 1989; Girdler et al., 1992; Ravat et al., 2002; Ouabego et al., 2013; Njiteu et al., 2021a) produced a variety of models on the origin of the BMA and thus, the controversy around this anomaly. A recent study (Njiteu, 2022) in contrast indicated a geological and probable crustal origin of the anomaly. So, it would be justified to question the presence and extension of geological structures whose physical characteristics (magnetic and thermal) would help to define such an anomaly. Ouabego et al. (2013) interpreted that the observed magnetic anomaly could be caused by the central African itabirites (metamorphosed banded iron formations), which possess the high magnetic susceptibilities. Since the itabirites occur within the greenstone belts, this makes them a leading candidate in defining the sources of this anomaly. Boukeke (1994) suggested that granulites (high P – T° rocks) are likely to be rooted some 50 km below the northern edge of the Congo Craton and Boukeke (1994), Dorbath et al. (1985) and Njiteu et al. (2021b) showed that there is a spatial relationship between the BMA, the resultant and the magnetic susceptibility bodies beneath the northern edge of the Congo Craton (Fig. 2C). Launay et al. (2018) indicated that the BIFs are the source of a similarly sized west African magnetic anomaly, which occurs at the edges of the West African Craton. The greenstone belts which are exposed at northern edge of the Congo Craton in Cameroon (Fig. 3B; Akumbom et al., 2022; Ndime et al., 2019; Tessontsap et al., 2017; Poidevin, 1991) are 1–2 km thick (Alexandrov et al. 1973) with the southern portion of the BMA (Figs. 1a-b). In the Central African Republic, the greenstones belt extends over a distance of 150–250 km (Dostal et al., 1985) and consist of mafic to ultramafic lithologies occurring in synclines, itabirites and metarhyolites (Fig. 3A). The BIFs have been dated between 2 and 3.8

Ga, with most occurring around 2.5 Ga. Younger BIFs have been reported between 0.5 and 1Ga (Klein, 2005) and predominantly composed of quartz, magnetite and hematite. By considering the magnetic signals specific to this anomaly and its geotectonic context, this study attempts, on the basis of simple direct models, to reconstruct with acceptable margins the probable sources of the anomaly.

4. Gravity and magnetic data

Ground gravity data in the form of simple Bouguer gravity anomalies were obtained from the International Gravimetric Bureau and were collected during several campaigns in Cameroon, Central African Republic and bordering countries along tracks and roads by the Institute of Research for Development (IRD) - formerly known as ORSTOM (Office for Scientific and Technical Research in the Overseas Territories). The gravity stations are spaced about 3 to 10 km apart (Godivier et al., 1986; Poudjom et al., 1995). In Cameroon, the error of the station coordinates varies between 0,1' and 1' (200 and 2000 m) and the accuracy of the gravity values is estimated to be approximately 0.2 mGal (Poudjom et al., 1995). In Central African Republic, the maximum error on the position of the measurements is estimated to be 200 m, 10 m on the elevation and less than 1 mGal on the gravity measurements (Boukeke et al., 1995). The database contains 33, 085 stations (Fig. 5) with some local areas having better coverage than others because of limited access due to the landscape and dense forest. Since the g-value on the ground is a superposition of several effects, undesirable effects (topography, instrumental drift) must be reduced. Variations in altitude also cause the g-value to vary, so it is important to bring the measured values back to the same reference level in order to make comparisons. It is assumed that each measurement made at an altitude (h) can be brought back to the level of the geoid (Z = 0) or to any reference point parallel to the geoid and whose altitude is expressed by Z = H (Poudjom 1993; Boukeke, 1994). If we consider g, the value read at a station and h, its altitude with respect to a geodetic reference frame, then the value g0 at this equipotential surface is expressed by:

$g_0 = g + 0.3086h$ (1)

This correction reduces the gravity value measured at the geoid by 0,3086 mGal/m. The free-air correction does not take into account the mass that may exist between the measuring station and the geoid. For the calculation of the anomaly (difference between a measured value and a theoretical value realised at the same measurement point and for the same geophysical parameter, i.e., density), it is important to calculate the theoretical value of g. For a homogeneous ellipsoid model defined by: the major axis half-axis of the ellipsoid: a = 6378160 m, the minor axis half-axis of the ellipsoid: b = 6356774,5 m, the ellipticity: e = (a-b) / a = 1/298,247, the product GM = 398603*109 m^2/S^2, the theoretical value of gravity g_T will depend only on the latitude φ and will be computed according to the relation (2):

$g_T = 978{,}031850\,(1 + 0.005278895\sin^2\varphi + 0.000023462\sin^4\varphi)$ (*2*)

Consequently, the free-air gravity (Fig. 4) is calculated by subtracting the g_T value from the first relation:

$\Delta gl = g + 0.3086h - g_T$ (3)

By comparing the spatial distribution of free-air anomalies and topography, we find that the high altitudes regions (Fig. 1B) are characterized by positive free-air anomalies.

Correlation between the free-air anomalies and the topography (Fig. 8) help to predict the state of isostatic equilibrium; Poudjom et al. (1992); Njiteu et al. (2021b), showed that relatively low regions (Fig. 1B; with altitudes less than 750 m or even 1000 m) where the free-air anomaly is almost null (Fig. 4), are roughly in isostatic equilibrium. However, in higher altitude areas (Fig. 1B; more than 1000 m), the free-air anomaly depends strongly on the topography (Fig. 8). More the free-air anomalies follow a similar direction with those defined by the large deformation corridors: the Central Cameroon shear zone, the Tchollire-Banyo shear zone and the Cameroon Volcanic Line respectively ENE and NE (Fig. 4). The complete Bouguer gravity anomaly (CBA) was calculated using a constant density of 2670 kg/m^3 and mean sea level as a datum. Gravity terrain correction were applied using a digital elevation model (DEM) from 0°-22N and 5°-50°E and a terrain density of 2670 kg/m^3 to compute a complete Bouguer gravity anomaly. The CBA data were gridded using minimum curvature at 3 km interval to produce a complete Bouguer gravity anomaly map (Fig. 5). The analysis of the evolutionary trend between the CBA and the topography along the selected profiles (Fig. 8) shows two cases: generally, following a N-S orientation, an inverse correlation towards the South, i.e., in the Precambrian terrains of Cameroon and Central Africa (Fig. 3A). This trend reflects the rigidity of the lithosphere with elastic thickness values ranges between 100 and 150 km (Njiteu et al., 2021b; Audet and Bürgmann, 2011; Gussinyé et al., 2009); These values correspond to a thick continental crust (40 km; Tokam et al., 2010; Njiteu et al., 2021a; Gallacher and Bastow, 2012). Towards the north of the profiles (Fig. 8), i.e., in the rift zones (Fig. 2C), a positive correlation between topography and Bouguer is observed, indicating a less rigid lithosphere. Moreover, according to Njiteu et al (2021b), the elastic thickness values in these areas vary between 20 and 100 km; the crust being less thick and constantly remobilised due to the seismic and thermo-tectonic events in connection with the regional shear zones and the Cameroon volcanic line (Fig. 1B).

The magnetic data were derived from the third version of the Global Earth Magnetic Anomaly Grid (EMAG2-v3) which is a compilation of ground, satellite, marine and aeromagnetic data where wavelengths of more than 330 km have been replaced with the magnetic anomalies from the lithospheric MF7 CHAMP satellite model (Meyer et al., 2017). The EMAG2-v3 has resolution of 2-arc-minutes and the elevations have been downward continued to 4 km above sea level (Meyer et al., 2017). Compared to the EMAG2-v2 database (Maus et al., 2009) which predicted magnetic anomalies based on the local geology for the interpretation of anomalies in the areas where there is no available data, the third version is based only on available datasets (Meyer et al., 2017). The EMAG2-v3 better represents the complexity of the anomalies and reflects more precisely the regions where no data have been collected. A total magnetic intensity (TMI) data were gridded at 10 km spacing grid and shown in Fig. 6.

To remove the dipolar nature of the earth's magnetic field, one normally uses the reduction to the pole (RTP) operator (Keating and Zerbo, 1996; Luo et al., 2010; MacLeod et al., 2013; Zhang et al., 2018) on the

data. However, RTP is unstable at low latitudes and one can apply a latitude correction to overcome this difficulty. The TMI data (Fig. 6) were reduced to the north magnetic pole with an average inclination of 8°, declination of -3° and an amplitude correction of -82°. The RTP data were gridded at a 10 km interval using the minimum curvature method to produce a RTP magnetic anomaly map (Fig. 7).
The CBA map (Fig. 5) has anomalies that range between − 10 and − 110 mGal in value. The region north of the BMA has higher amplitude anomalies that reflect thicker crust, while within the BMA region, the anomalies are of lower values with short wavelengths reflecting the Proterozoic and Archean lithological changes.

As compared to the RTP map (Fig. 7), the gravity anomalies are reflecting different lithologies mainly related to Congo Craton structures. In the Central African Republic, the BMA mainly occurs over Precambrian lithologies, extending parallel to the cratonic structures in southern Cameroon beneath the E-W trending transition zone delineating the Congo Craton and the Adamawa uplift (Fig. 2C). The spatial extent of the magnetic anomaly indicates that these sources are closely related to the greenstone belts including BIFs in the Congo Craton, which are associated with the granulites (Fig. 3A). Considering nine profiles (Fig. 1B), an overview of the different field strength variations is given in Fig. 8.

5. Curie isothermal depths beneath the BMA

The estimation of the magnetization limit is one parameter to determine the nature of the potential magnetic sources of the BMA. This limit represents the depth beyond which rocks lose their ferromagnetic or ferrimagnetic properties due to temperatures above their Curie point. An estimation of the Curie isothermal depths is one of the main steps allowing to approximate the thermal state of the crust (Quintero et al., 2019; Elbarbary et al., 2022). Knowledge of the Curie isothermal depth variations also provides information on the different geological discontinuities which may be due either to the regional variations in the mineralogical composition of rocks or the variations in the local or regional geothermal regime. Njiteu et al. (2021a) used spectral methods (Spector et al., 1970; Shuey et al., 1976; Tanaka et al., 1999; Tanaka et al., 2017) to determine the Curie isothermal depths of the BMA and the surrounding region. Their analysis estimated that the maximum depth of magnetization ranged between 11 and 35 km (Njiteu et al., 2021a) and trend approximately in an ENE-WSW direction (Fig. 9). The depths increase from west to east, with the shallowest depth being under the CVL and the deepest regions being under and along the edge of the Congo Craton. To help understand the nature of these depths, crustal thickness values determined from seismic receiver functions from 32 seismic stations in Cameroon (Tokam et al., 2010; Gallacher and Bastow, 2012) are shown (Fig. 9). The seismic depths also increase toward the east, with values of nearly 40 km at the northern edge of the Congo Craton. The northern edge of the Congo Craton is below the BMA, where the Curie depth are between 36 and 42 km. These depths give us an idea of the size of the magnetization source causing the BMA. The deeper Curie depths are common in cratonic areas in Africa (Mohamed & Al Deep, 2021).

6. Magnetic map analysis

The magnetic data were analysed using analytic signals (AS) (Macleod et al., 2013), horizontal gradients (Blakely and Simpson, 1986; Blakely, 1996); and tilt derivatives (Nabighian et al., 2005; Salem et al., 2008). The derivative methods are useful in determining the lateral boundaries of magnetic susceptibility bodies with the vertical derivatives being good at determining the width of the body and the horizontal derivatives being good at determining the lateral edges (Marson and Klingele, 1993). However, these derivative methods provide only a first-order geological interpretation (Grauch and Cordell, 1987) with the results often contaminated by nearby sources and non-vertical source edges. While all derivative techniques will indicate the position of a body, we used the horizontal derivatives which is better suited in locating or enhancing the edge of a body than vertical derivatives (Cordell, 1979; Blakely and Simpson, 1986). However, horizontal derivatives will produce a large range of lineaments from both shallow and deep sources, making the interpretation difficult (Demissie et al., 2018). To overcome this problem, AS and tilt derivatives can aid in determining the nature of the lineaments. The AS method is calculated from total derivatives and may generate maximum anomalies over the edges of magnetic susceptibility body and works well on shallow source bodies (Li, 2006). The AS method should be combined with a horizontal derivative map to indicate which maxima are related to vertical contacts, as the horizontal derivatives produce linear anomalies that are commonly continuous, while the AS method produces more circular anomalies that are less continuous (Phillips, 2000). However, the AS solution is more accurate and if the HDR and AS solutions overlie each other, then the contact is vertical (Phillips, 2000). If the HDR contacts are offset from the AS contacts, then the contacts are dipping (Phillips, 2000).

The tilt derivative method which is ratio of vertical to horizontal derivative, and does not have the problem of producing anomalies from deep and shallow sources (Salem et al., 2008). The tilt derivative results are called the tilt angle where a positive tilt angle represents tilt variations within a magnetic susceptibility source, negative values are tilt variations outside a source and zero values represent the edges of a magnetic susceptibility source (Salem et al., 2008). The AS, horizontal derivative and tilt derivative maps using the RTP data are shown in Figs. 11–13, respectively.

On the AS map (Fig. 10A), the anomalies over the BMA can be broken into three regions (1–3, Fig. 10A). In Cameroon (region 3), the anomalies have short wavelengths and trend roughly N-S with some trending E-W. These anomalies are located at the northern edge of the Congo Craton. In the Central African Republic, the anomalies trend N-S to NW-SE (region 2, Fig. 10A) and Boukeke (1994) indicated that these directions correspond to the transition zone between the Congo craton and the mobile zone. Region 1, located in the Central African Republic, shows a circular anomaly but on a closer inspection, it is composed of short wavelength anomalies-oriented NW-SE and E-W. The NW and SE directions may be related to Archean greenstone belts containing granulites and itabirites (Poidevin et al., 1981). The rough E-W trending anomalies may be related to the shear zones (Figs. 2 and 10A).

The horizontal derivative map (Fig. 10B) more clearly defines the linear anomalies than the AS map. The BMA is associated with mainly E-W directions with the majority of these lineations being basically in the same locations as most of the AS anomalies suggesting that the magnetic susceptibility bodies causing the anomalies are vertical. Girdler et al. (1992), Ravat et al. (2002) and Klokocnik et al. (2010) have

shown that the BMA in the Central African Republic may be linked to a meteorite impact (Fig. 3A) that has a circular aureole over a radius equal to the size of the anomaly between eastern Central African Republic and the borders with Cameroon and adjacent countries (Fig. 3A). However, the circular anomaly observed from the AS map (Fig. 10A) is too localized and is really a combination of smaller wavelength anomalies. The magnetic sources within region 1 may be a mafic intrusion or a magnetite – enriched metamorphic aureole. The fact that the shape of the anomalies constituting the BMA vary from one derivative map to another undoubtedly suggests that the magnetic susceptibility and even the magnetic remanence should be considered in quantifying the sources.

The tilt derivative map (Fig. 10C) shows approximately the same lineation orientations as those on the horizontal derivative map (Fig. 10B), with most lineations oriented E-W and ENE-WSW. The ENE-WSW trending lineations are related to the regional shear zones affecting the Pan-African basement. This direction is along to the major axis of the BMA, which implies a setting in favour of a regional tectonic constraint. The E-W trending lineaments are that of the secondary gradients related to lithological variations within the Pan African lithologies north of the Congo Craton (Fig. 3A). The tilt-derivative lineations indicate that at the parallel 4°N in Cameroon, the BMA is parallel with the Congo Craton northern limit (Boukeke, 1994; Ngatchou et al., 2014; Ghomsi et al., 2020).

7. Forward modelling

In order to aid in constraining the depth, geometry and physical properties of the BMA source, nine two-dimensional (2-D) forward models (Figs. 11a-i) were constructed using the topography (Fig. 1B) magnetic and complete Bouguer gravity anomaly data (Figs. 5, 7, 9 and 10). To constrain the depths, shape and physical properties of the bodies along each profile, constraints including geological mapping, broadband seismic models and average physical property values from previous studies (Telford et al., 1990; Hemant, 2003; Tadjou et al., 2009) were used. There are no known density or magnetic susceptibility measurements in the region and no seismic refraction studies where densities could be estimated from P-wave values. Additionally, there are no deep drill holes to estimate the depth to the various Proterozoic and Archean lithologic units. Thus, the forward models will be only constrained from widely spaced broadband seismic models to estimate the depth of the crust-mantle and upper-lower crust boundary. Tokam et al. (2010); Gallacher & Bastow (2012); Njiteu et al. (2021b) determined the crustal thicknesses (Fig. 11a-i) varied between 37–42 km which are similar to the bottom of the magnetic susceptibility bodies estimated for Curie depths along each profile (Fig. 9). The constraints were varied by 10% during the modelling process to create final geological reasonable gravity/magnetic models.
The three main bodies on each profile are the upper, middle and lower crusts with densities of 2670 kg/m^3, 2850 kg/m^3 and 3000 kg/m^3 respectively. At the start of the modelling process, these three bodies are considered as non-magnetic. The observed anomalies were sampled along each profile at a constant 5 km spacing. The spacing between the profiles is a constant 146 km. Profiles are taken long enough to provide good coverage of the magnetic sources and thus minimize border effects. The magnetic parameters of the bodies included a total magnetic intensity of 33,812 nT, inclination of 90° and a

declination of 3°. The crustal structure was determined based on gravity (Fig. 5) and topographic data (Fig. 1B). The shape and extension of the intrusions depended on the densities and magnetic susceptibilities of each body was necessary to fit the observed data. The bottom of the majority of the magnetic sources varies accordingly with the ~ 35 km Curie depths estimated along the BMA (Fig. 9). Models P1 to P4 passes through the E-W trending gravity maximum in southern Cameroon (Fig. 5). All the bodies in the crust have a density of 2850 kg/m^3 which is compatible with granulites (Telford et al., 1990; Boukeke, 1994; Tadjou et al., 2009; Hemant, 2003). The magnetic susceptibilities values for the crustal bodies along models P1 and P2 (0.06 SI and 0.1 SI) are characteristic of basic granulites (Telford et al., 1990). Magnetic susceptibilities values along profiles P3, P5 and P7 are interpreted to be metamorphic rocks enriched in magnetite. On models P4, P8, the magnetic maxima are modelled due to BIFs. Considering their high hematite and magnetite enrichment, BIFs have mineralogical characteristics compatible with intense magnetism and as such, depending on their abundance in the crust, they are likely to perturb field values. The conditions to be considered are both the position of the outcrops and the magnetic properties observed in the field. The location of the BIFs deposits in the Congo craton (Fig. 3A) allows a spatial correlation with the BMA. Ouabego et al. (2013) showed that over an area of 15,000 km^2, the itabirites in the Central African Republic have the highest magnetic susceptibility values. Alexandrov (1973) using the anomalies in the Kursk region of Russia, with amplitudes of 10,000 nT, showed that the anomalies are associated with Precambrian BIFs formations; which extend discontinuously across the surface for about 3000 km. For models P6 and P9, the surface geology does not indicate what the source may be but that there is a large magnetic susceptibility body within the crust.

8. Discussion

The magnetic data analysis shows that the BMA is a large amplitude magnetic anomaly on the northern edge of the Congo Craton along the CAOB (Fig. 2C). The BMA is not one large, continuous anomaly but consists of several superimposed individual anomalies that compose the large amplitude anomaly (Figs. 10A-C). The anomalies are associated with Pan African aged NE-trending regional shear zones and E-trending lineaments. Modelling indicates that the high magnetic susceptibility bodies start to the south of the BMA, at the northern edge of the Congo Craton and end at the southern edge of the Saharan Metacraton (Fig. 2C). The derivative analysis (Figs. 10A-C) and 2D forward modelling (Figs. 11A-I) support that the BMA is of geological origin caused by tectonic processes and the magnetic susceptibility bodies are located within mainly the middle and lower crust. The gravity anomalies over the same region contain gravity maxima which have dense sources in some locations but there are numerous regions with gravity minima (Braitenberg et al., 2015; Fig. 5). This suggests that magnetic minerals that cause the BMA occur in low density rocks. Thus, the BMA anomaly, which in its spatial extension covers the northern edge of the Congo Craton and CAOB (Fig. 2), has a bipolar structure whose sources have high magnetic susceptibilities, relatively dense in places and consist of deeply buried rocks that are stable under high P-T° conditions.

Analysis of the magnetic lineaments on the horizontal derivative (Fig. 10B) and tilt derivative (Fig. 10C) maps indicates that the BMA consists of mostly NE-SW trending anomalies with several E-W trending secondary anomalies. There is a spatial correlation between the major E-W and NE-SW tectonic directions along the regional shear zones (Fig. 2) with the magnetic lineaments. These correlations are also indicative of the tectonic control on the emplacement of the rocks beneath the BMA. The analysis of the mechanical behaviour of the lithosphere (Njiteu et al., 2021) shows the influence of regional tectonics on the crustal architecture in this region.

If one accepts the link between the geological structures at the northern edge of the Congo Craton and the BMA, and its subsequent significant vertical extension, then a fundamental hypothesis can be formed based on the models (Fig. 11a-i). This includes the existence of wide spread BIFs in Central Africa (Dostal et al., 1985; Ndime et al., 2019) and the presence of granulites at the northern edge of the Congo Craton (Pin and Poidevin, 1987; Boukeke, 1994; Toteu et al., 2006). The complete Bouguer gravity anomalies (Fig. 5) show an elongated E-W maximum in Cameroon that have been interpreted to be caused by buried granulites (Boukeke, 1994; Tadjou et al., 2009). The crust between Cameroon and the Central African Republic is mainly influenced by several middle to lower crustal high magnetic susceptibility bodies which are also dense and can explain the gravity maxima at the northern edge of the Congo Craton and the BMA. The location of the nine profiles (Fig. 1B) depends of the orientation of the magnetic gradient (Figs. 10A-C). The regional tectonic directions and orientation of the magnetic gradients are criteria that defined the choice of the profiles. in the intra-continental domain, Cameroon and Central African Republic, the BMA extends over a distance of roughly 1540 km (Fig. 7), with secondary E-W gradients (Fig. 10A-C). Along profiles P1, P2, P3 and P4, the modeled magnetic susceptibility sources are elongated bodies with a density of 2850 kg/m^3 at the northern edge of the Congo Craton. This result is consistent with previous studies Boukeke, (1994) and Tadjou et al., (2009), supporting the presence of middle to lower crustal granulites. The magnetic susceptibility values, which range from 0.6 to 0.1 SI, show that these granulites contain significant magnetic minerals and are located at depths between 14 and 28 km. The modelling indicated also that the magnetic granulites are not isolated sources, as Poidevin (1987) has shown there is a large distribution of granulites with iron oxides at the northern edge of the Congo Craton. These granulites are aligned with the BIFs and metamorphic rocks (Giorgi et al., 1990; Poidevin, 1991; Tetsontsap et al., 2017; Ndime et al., 2019). However, there is a large misfit between the observed and calculated magnetic anomalies on models P7 and P8 (Figs. 11G-H) that may be caused by the complexity of the BMA where remanent magnetization may be a component of the magnetization. Magnetic models in the Bangui area indicated that either metamorphic rocks, BIFs or both rock types could be the sources of the BMA. Recently Lemenkova and Debeir (2023) shows good correspondence between the spatial distribution of greenstone belts, metamorphosed basalt, granites and the BMA in the Central part of the Central African Republic.

The results of this study, suggests that there are different lithologies as potential sources of the BMA and agree with Galdeano (1981) who showed, through a Gondwanian reconstruction, that along the northern Congo Craton and the CAOB consists of a probable continuity of mafic and ultramafic sources based the

P and T° conditions were part of the lower crust to upper mantle. Recent geochemical and isotopic analyses (Toteu et al., 2022) have been used to infer that the interaction of northern edge of the Congo craton with the southern edge of Saharan Metacraton was related to two north dipping subduction zones during the Pan African orogeny. This interaction caused island arcs that were accreted to the Saharan Metacraton and the latest collision (620 – 550 Ma) between the two cratons created several shear and suture zones (including the Raghane shear zone in the west, the CAOB in the south and the Keraf-Kabus-Sekerr in the east). Magmatism also occurred during the creation of these shear and suture zones, producing deep crustal migration of fluids that may have been the source of the magnetic minerals within the granulites (Toteu et al., 2022). Our models, which show that the magnetic susceptibility sources must be deep (as deep as 35 km) and that these sources cover the middle to lower crust. Additionally, the high magnetic susceptibility bodies occur only between the boundaries of the Congo Craton and the Saharan Metacraton suggesting that they were formed during collision between the two cratons during the Pan African orogeny and that the magnetic minerals may be related to magmatic events during the latest stages of the Pan African orogeny. Given the above tectonic model, our magnetic and gravity models indicate provide additional evidence that crust at the northern edge of the Congo Craton including the CAOB was formed by some type of collision event that involved the entire crust and maybe the upper mantle. This tectonic scenario is similar to the Mozambique belt in East Africa, where the collision of terranes with the Saharan Metacraton during the Pan African orogeny involved middle and lower crustal rocks (Kroner and Stern, 2005).

8.1. Limitation of known models over the BMA area and speculations

Five major cratonic regions are known on the African continent. They include the Northwest, Northeast, North Central and South regions. The BMA is among the largest and most intense lithospheric anomalies. However, studies on potential magnetic sources are still limited. There are a variety of models to explain this anomaly and specify the parameters of its source(s) (Ravat, 1989; Regan and Marsh, 1982; Girdler et al., 1992; Ouabego et al., 2013). Large uncertainties remain in the absence of overriding constraints. The magnetic properties, extend, depth and nature of these sources are still highly debatable. Considering the lack of direct information on the geodynamic environment of the deep rocks, the uncertainty on the structure of the lower crust at the level of cratons, various attempts to model magnetic sources are difficult due to the lack of reliable constraint in parallel with the magnetic data. In order to know the optimal magnetic characteristics of the modelled bodies, it is useful to have experimental input in rock magnetism. According to Gidler et al. (2004) this would help to understand how the variation of physical parameters with depth could affect the rocks. Several unconstrained models have been developed so far according to Regan and Marsh (1982); Dorbath et al. (1985); Boukeke (1994); Ouabego et al. (2013). To explain the BMA, Regan & Marsh (1982) proposed a model of deep intrusions. The Precambrian rocks of the Central African Republic are distinguished by a granite-gneissic and charnockite base complex on which epimetamorphic series are superimposed. In the centre of the Central African Republic, these series constitute the Oubangui basin, interpreted as a synclinorium comprising several sub-basins (Boukeke,

1994). Thus, the BMA would be superimposed on the Oubangui basin, which is also marked by a large negative gravity anomaly of about − 80 mGals (Lemenkova and Debeir, 2023). The hypothesis on the source of the anomaly deduced by Regan and Marsh (1982) was made taking into account the superposition of the two anomalies on the Oubangui basin. This would indicate the presence of a crustal intrusion whose (1) magnetic properties would generate the anomaly; (2) overloading of the intrusive body would cause a crustal root that would explain the negative gravity anomaly. Three components were thus deduced from the calculated model: the charnockitic crustal enclosure; the intrusive body and the surface formations of the basin. This work is just an indicator of the average characteristics of the sources of the anomaly (Boukeke, 1994). Following a NW profile in the Central African Republic, Dorbath et al. (1985) inverted the seismic data: this showed a variation in seismic velocities below the anomaly. The area of high seismic velocities was correlated with the dense and magnetic body deduced by Regan and Marsh (1982). Boukeke (1994) through geological comparisons shows that these high velocities estimated between 40 and 120 km mark internal discontinuities in the Congo Craton. Thus, there would be no link between these discontinuities and the probable body beneath the BMA. Boukeke (1994) proposes an interpretative model in relation to the Gondwana interpretations after Galdeano (1981). According to these authors, the sources of BMA are probably deep, mafic to ultramafic rocks, stable at the P - T° conditions of the lower crust and upper mantle. However, none of the above models take into account (1) the influence of the Central African iron deposits; (2) the impact of remanence is neglected; (3) most of these models have a limited spatial extension over the whole anomaly - there are no models to correlate the gravity anomalies of the northern edge of the Congo Craton and the BMA. Ouabego et al. (2013) around the Bangui region proposed a crustal model that combines the susceptibility and natural magnetic remanence of rocks, showing BIFs as good candidates with a Koenigsberger ratio greater than 1. However, these models remain highly debatable as the sources are not unique. According to Ouabego et al. (2013) BIFs would be a likely issue to explain the Anomaly. Recently Launay et al. (2018) showed the BIFs as a good candidate to explain the West African Magnetic Anomaly. Another limitation is the lack of constraints on the magnetic composition of the lower crust and upper mantle. The lithosphere - asthenosphere boundary in the region is not clearly defined. The possibility of iron xenoliths in the lower mantle has been reviewed by Ferre et al. (2020) who showed the thermal stability of some iron oxides as well as their magnetic remanence at a depth of about 660 km. Thus, analysing the contribution of the mantle as a source of BMA should be consider. According with the present results (Figs. 11A-I) and the developments over the West African magnetic Anomaly (Launay et al., 2018) the latest issue (Ferre et al., 2020) seems to be a good perspective.

9. Conclusions

A magnetic and gravity analysis of the Bangui magnetic anomaly (BMA) and surrounding regions was conducted to understand the origin of the BMA. The BMA is one of the largest continental magnetic anomalies in terms of amplitude and lateral size on Earth. The analysis consisting deriving derivative magnetic anomaly maps and 2-D gravity and magnetic forward models were constrained by geological and broadband seismic studies. Using a Curie isothermal analysis, the depth of the magnetic

susceptibility sources ranged from 15–35 km and were used in creating gravity and magnetic forward models. Previous studies have shown that the BMA may be related to Archean Congo Craton structures and the above analyses have shown that the BMA anomalies are mainly concentrated at the between the northern edge of the Congo Craton and the southern edge of the Saharan Metacraton. Nine magnetic and gravity forward models across the BMA that crossed the E-W trending gravity and magnetic maxima were selected to model the crustal lithology. The results of the map analysis and forward modelling indicated that the magnetic susceptibility sources that created the BMA are not one large body but a series of magnetic susceptibility sources. The derivative analysis and 2D forward models, indicated that these sources are elongated. They extend from 2 km to ~ 35 km in depth, with an average density of 2850 kg/m^3 and magnetic susceptibilities between 0.06–0.25 SI. The modelling bodies occur mainly in the middle and lower crust beneath the CAOB. Based on surface geological studies these bodies may be related to magnetic mineral rich granulites and banded iron formations. Such a highly magnetic may be related to a probable fluid circulation from magmatic events during the latest stages of the Pan African orogeny. This result could be linked to a deep-seated hydrothermalism phenomenon that occurred during the various orogenic episodes recorded in Central Africa.

Declarations

Acknowledgements

C.D. Njiteu thanks the Institute of Research for Development (IRD) for the help in the acquisition of ground gravity data used in this study. This research did not receive any specific grant from funding agencies in the public, commercial, or not-for-profit sectors.

Competing Interests

The authors declare that they have no competing interests.

References

1. Abdelsalam, M. G., Liegeois, J. P., & Stern, R. J. (2002). The Saharan metacraton. *Journal of African Earth Science.* 34, 119–136. https://doi.org/10.1016/S0899-5362(02)00013-1
2. Akumbom, V., Ilouga, I. C., Bomyoymoah Ndzegha, B., & Cheo Suh E. (2022). Petrology of banded iron formation-related country rocks at the northern limit of the Mbalam iron ore district, southeastern Cameroon. *Journal of the Cameroon Academy of Sciences*, 18:2. https://dx.doi.org/10.4314/jcas.v182.5
3. Alexandrov, E. A. (1973). The Precambrian banded iron formations of the Soviet Union. *Econ. Geol.* 68, 1035–1062. https://doi.org/10.2113/gsecongeo.68.7.1035
4. Audet, P., & Bürgmann, R., 2011. Dominant role of tectonic inheritance in supercontinent cycles. Nature Geoscience, *Letters*. https://doi.org/10.1038/NGEO1080.

5. Braitenberg, C. (2015). Exploration of tectonic structures with GOCE in Africa and across-continents. *International Journal of Applied Earth Observation and Geoinformation*, 35, 88–95. https://doi.org/10.1016/j.jag.2014.01.013
6. Braitenberg, C., Mariani, P., Ebbing, J., & Sprlak, M. (2011). The enigmatic Chad lineament revisited with global gravity and gravity-gradient fields. *Geological Society, London, Special Publications* 357 (1), 329–341. https://doi.org/10.1144/sp357.18
7. Benkova, N. P., Dolginow, S. S., & Simonenko, T. N. (1973). Residual magnetic field from the satellite Cosmos 49. *Journal of Geophysical Research*, 78, 798-803.
8. Blakely, R. (1996). Potential theory in gravity and magnetic applications. *Cambridge University Press*, 461p.
9. Blakely, R., & Simpson, W. (1986). Approximating edges of sources bodies from magnetic or gravity anomalies. *Geophysics*, 51(7), 1494-1498.
10. Boukeke, D. B., Legeley-Padovani, A., Poudjom Djomani, Y., Foy, R., & Albouy, Y. (1995). Levés gravimétriques de reconnaissance, gravity map, République Centrafricaine. *Edition ORSTOM (Institut Français de Recherche Scientifique pour le Développement en Coopération)*. 37p.
11. Boukeke, D. (1994). Structures crustales d'Afrique Centrale déduites des anomalies gravimétrique et magnétique : le domaine Précambrien de la République Centrafricaine et du Sud-Cameroun. *Thèse de Doctorat PhD, Université de Paris Sud, Centre Orsay, ORSTOM*, 278p.
12. Clark, D. A. (1999). Magnetic petrology of igneous intrusions: Implications for exploration and magnetic interpretation. *Exploration Geophysics*, 30, 5-26.
13. Cordell, L. (1979). Gravimetric expression of graben faulting in Santa Fe County and the Espanola Basin, New Mexico, in R. V. Ingersoll, ed. Guidebook to Santa Fe County: *30th Field Conference, New Mexico Geological Society*, 59-64.
14. Demissie, Z., Mickus, K., Bridges, D., & Abdelsalam, M. (2018). Upper lithospheric structure of the Dobi graben, Afar Depression from magnetics and gravity data. *Journal of African Earth Sciences* 147, 136-151.
15. Dorbath, C., Dorbath, L., Floc'h, H., Mauplot, J. P., & Rouyre, P. (1981). Campagne d'enregistrement sismologique sur l'anomalie magnétique de Bangui. *ORSTOM*, 11p.
16. Dorbath, C., Dorbath, L., Gaulon, R., & Hatzfeld, D. (1985). Seismological investigation of the Bangui magnetic anomaly region and its relation to the margin of the Congo craton. *Earth and Planetary Sciences Letters*, 75, 231-244.
17. Dostal, J. Dupuy, C., & Poidevin, J. (1985). Geochemistry of Precambrian basaltic rocks from the Central African Republic (Equatorial Africa). *Canadian Journal of Earth Sciences*, 22, 653-662.
18. Elbarbary, S., Mohamed Abdel, Z., Saibi, H., Abdel-Rahman, F., Ravat D., & Marzouk H. (2022). Thermal structure of the African continent based on magnetic data: future geothermal renewable energy exploration in Africa. *Renewable and Sustainable Energy Reviews*, 158, 112088. https://doi.org/10.1016/j.rser.2022.112088

19. Eyike, A., & Ebbing, J. (2015). Lithospheric structure of the West and Central African Rift System from regional three-dimensional gravity modelling. *South African Journal of Geology*, 118, 285–298. https://doi.org/10.2113/gssajg.118.3.285
20. Ferre E., Ilya Kupenko, Fatima M. H., Ravat D. and Carmen S. (2020). Magnetic sources in the Earth's mantle. *Nature Review*, 11p.
21. Fairhead, J. D., & Okereke, C. S. (1987). A regional gravity study of the West African rift system in Nigeria and Cameroon and its tectonic interpretation. *Tectonophysics*, 143(1–3), 141–159. https://doi.org/10.1016/0040-1951(87)90084-9
22. Feybesse, J. L., Johan, V., Triboulet, C., Guerrot, C., Mayaga-Mikolo, F., Bouchot, V., & Eko N'dong, J. (1998). The West Central African belt: a model of 2.5-2.0 Ga accretion and two-phase orogenic evolution. *Journal of African Earth Sciences*, 87, 161-216.
23. Galdeano, A. (1981). Les mesures magnétiques du satellite Magsat et la dérive des continents. *Comptes Rendus de l'Académie des Sciences de Paris*, 293, Série II, p. 161-164.
24. Gallacher, R. J., & Bastow, I. D. (2012). The development of the Cameroon Volcanic Line: evidence from teleseismic receiver functions. *Tectonics* 31. http://dx.doi.org/10.1029/2011TC003028
25. Genik, G. J. (1993). Petroleum geology of Cretaceous-Tertiary rift basins in Niger,Chad, and Central African Republic. *The American association of petroleum geologists bulletin*, 77(8), 1405–1434.
26. Ghomsi, F. E., Nguiya, S., Mandal, A., Enyegue, A. N., Tenzer, R., Tokam Kamga, A. P., & Nouayou R. (2020). Cameroon's crustal configuration from gravity and topographic models and seismic data. *Journal of African Earth Sciences*, http://dx.doi.org/10.1016/j.jafrearsci.2019.103657
27. Gidler, S., Le Golf M., Peyronneau, J., and Chervin, J. C. (2004). Magnetic properties of single and multi-domain magnetite under pressure from 0 to 6 GPa. Geophysical Reasearch Letters, 31. https://doi.org/10.1029/2004GL019844.
28. Girdler, R. W., Taylor, P. T., & Frawler, J. J. (1992). A possible impact origin for the Bangui Magnetic anomaly (Central Africa). *Tectonophysics*, 212, 45-58.
29. Giorgi, L. Cornacchia, M., Vicat, J. P. Blondin, P. Babet, N., & Minot, J. B. (1990). Géochimie des métavolcanites de la ceinture de roches vertes de Bogoin-Boali, République Centrafricaine. *15th Colloquium of African Geology, Nancy I, Occas, Publ., 1990/20 CIFEG, Orléans (abstract)*.
30. Godivier, R., Legeley, A., & Albouy, Y. (1986). Levés gravimétriques de reconnaissance Congo-Gabon. *Editions ORSTOM, Institut Français de Recherche Scientifique pour le Développement en Coopération*. 17p.
31. Godivier, R., & Le Donche, L. (1962). Reseau magnetique ramené au 1er Janvier 1956. République Centrafricaine, Tchad Meridional. *Tectonophyics*, 212, 45-58
32. Godivier, R., & Vassal, A. (1980). Anomalie Magnétique en Centrafrique : un modèle géophysique. *Fonds Documentaire ORSTOM,* 9p.
33. Guiraud, R., & Binks, R. M. (1992). Chronology and geodynamic setting of Cretaceous-Cenozoic rifting in West and Central Africa. *Tectonophysics*, 213, 227–234.

34. Grauch, V. J. S., & Cordell, L. (1987). Limitations on determining density or magnetic boundaries from local horizontal gradients in gridded potential-field data: *72nd Annual International Meeting, SEG, Expanded Abstracts*, 762-765.
35. Gray, D. R., Foster, D. A., Maas, R., Spaggiari, C. V., Gregory, R. T., Goscombe, B., & Hoffmann, K. H. (2007). Continental growth and recycling by accretion of deformed turbidite fans and remnant ocean basins: Examples from Neoproterozoic and Phanerozoic orogens, In: Hatcher, R. D., Jr., Carlson, M. P., McBride, J. H., & Catalán, J. R. M. (Eds.), 4-D Framework of Continental Crust. *Geological Society of America Memoir* 63, pp. 63-92. 10.1130/2007.1200(05).
36. Gussinyé-Perez, M., Metois, M., Fernandez, M., Vergés, J., Fullea, J., & Lowry, A. R. (2009). Effective elastic thickness of Africa and its relationship to other proxies for lithospheric structure and surface tectonics. *Earth Planet Science*. Lett. 287, 152–167. https://doi.org/10.1016/j.epsl.2009.08.004
37. Haggerty, S. E. (2014). Carbonado diamond. Review of properties and origin. *Gems & Gemology*, 53, 168-179.
38. Hemant, K. (2003). Modelling and Interpretation of Global Lithospheric Magnetic Anomalies. *PhD Thesis, Freien University*, Berlin, 152p.
39. Keating, P., & Zerbo L. (1996). An improved technique for reduction to the pole at low latitudes. *Geophysics*, 61(1), 131-137.
40. Ki Kis, Taylor, P. T., Toronyi, B., & Puszta, S. (2021). Inversion of magnetic measurements of the Swarm A satellite of the Bangui Magnetic Anomaly. *International Journal of Magnetic and Electromagnetism*, 7:036. https://doi.org/10.35840/2631-5068/6536
41. Klokocnik, J., Kostelecky J., Novak P., & Wagner A. C. (2010). Detection of Earth impact craters aided by the detailed global gravitational model EGM2008. *Acta Geodyn. Geomater*. 7(157), 71-97.
42. Kroner, A., & Stern, R. (2005). Pan-African Orogeny*. Encyclopedia of Geology.* vol. 1, Elsevier, 1-12
43. Launay, N., Quesnel Y., Rochette P., & Demory, F. (2018). Iron formation as the source of the West African Magnetic crustal anomaly. *Frontiers in Earth Sciences*. 6, 32. https://doi.org/10.3389/feart.2018.00032
44. Lavreau, J., Poidevin, J., Ledent D., Liegeois, J.– P., & Weiss, D. (1990). Contribution to the geochronology of the basement of the Central African Republic. *Journal of African Earth Sciences*, 11, 69-82.
45. Lemenkova, P., & Debeir, O. (2023). Coherence of Bangui Magnetic Anomaly with topographic and gravity contrasts across Central African Republic. *Minerals*, 13, 604. https://doi.org/10.3390/min13050604
46. Lerouge, C., Cocherie, A., Toteu, S. F., Penaye, J., Milesi, J. P., Tchameni, R., Nsifa, N. E., Fanning, M. C., & Deloule, E. (2006). Shrimp U-Pb zircon age evidence for Paleoproterozoic sedimentation and 2.05Ga syntectonic plutonism in the Nyong Group, South-Western Cameroon: consequences for the Eburnean-Transamazonian belt of NE Brazil and Central Africa. *Journal of African Earth Sciences*, 44, 413-427.

47. Luo Yao, Xue, D., & Wang, M. (2010). Reduction to the pole at the geomagnetic equator. *Chinese Journal of Geophysics*, 53 (6), 1082-1089.
48. MacLeod, I. N., Keith, J., & Ting, D. (1993). 3D analytic signal in the interpretation of total magnetic field data at low magnetic latitudes. *Exploration Geophysics*, 24, 679-688.
49. Maddaloni, F., Pivetta, T., & Braitenberg, C. (2021). Gravimetry and petrophysics for defining the intracratonic and rift basins of the Western-Central Africa zone. *Geophysics*, 86(6), B369–B388. https://doi.org/10.1190/geo2019-0522.1
50. Marson, I., & Klingele, E. (1993). Advantages of using the vertical gradient of gravity for 3-D interpreation. *Geophysics* 58, 1588-1595.
51. Maus, S. et al. (2009). EMAG2. A 2-arc min resolution Earth Magnetic Anomaly Grid compiled from satellite, airbone and marine magnetic measurements. *Geochemistry, Geophysics and Geosystems*, 10, Q08005, https://doi.org/10.1029/2009GC002471
52. Marsh, B. D. (1977). On the origin of the Bangui magnetic anomaly, Central African Empire, NASA Report, 63p.
53. Meyer, B., Chulliat, A., & Saltus R. (2017). Derivation and error analysis of the Earth Magnetic Anomaly Grid at 2 arc min Resolution Version 3 (EMAG2v3). *Geochemistry, Geophysics and Geosystems*, 18, 4522-4537. https://doi.org/10.1002/2017GC007280
54. Milesi, J. P., D. Frizon de Lamotte, G. de Kock, & Toteu F. (2010). Tectonic map of Africa, 1:10 000 000 scale. *CCGM-CGMW, Paris*.
55. Mohamed, A., & Mohamed Al, D. (2021). Depth to the bottom of the magnetic layer, crustal thickness, and heat flow in Africa: Inferences from gravity and magnetic data. *Journal of African Earth Sciences*, 179, 104204. https://doi.org/10.1016/j.jafrearsci.2021.104204
56. Nabighian, M. N., Grauch V., Hansen R.O., LaFehr T., LiY. Peirce J., Phillips J. D., Ruder M.E. (2005). The historical development of the magnetic method in exploration. *Geophysics*, 70(6), 33-61.
57. Ndime Nzume, E., Ganno, S., & Zenti, J. P. (2019). Geochemistry and Pb-Pb geochronology of the Neoarchean Nkout West metamorphosed banded iron formation, southern Cameroon. *International Journal of Earth Sciences*, 108(5):1551-1570
58. Nedelec, A., Macaudiere, J., Nzenti, J. P., & Barbey P. (1986). Evolution structural et metamorphique des schistes de Mbalmayo (Cameroun). Implication pour la structure de la zone mobile panafricaine d'Afrique Centrale, au contact du craton du Congo. *Compte Rendu Académie des Sciences Paris*, 303, 75-80.
59. Ngalamo, G. J., Bisso, D., Abdelsalam, M., Atekwana, E., Andrew, B. K., & Ekodeck G. E. (2017). Geophysical imaging of metacratonization in the northern edge of the Congo Craton in Cameroon. *Journal of African Earth Sciences*, 129, 94-107.
60. Ngatchou, H. E., Genyou, L., Tabod, T.C., Kamguia, J., NGuiya, S., Tokam Kamga, A. P., & Xiaoping, K. E. (2014). Crustal structure beneath Cameroon from EGM2008. *Geodesy and Geodynamics*, 5 (1), 1–10. https://doi.org/10.3724/SP.J.1246.2014.01001

61. Njiteu, T. C. D., Basseka, C.A., Poudjom, D. Y., Sonia, R., Etame, J., Muriel, L., Seoane, L., Som Mbang, C., & Eyike A. (2021a). Crustal thickness, depth to the bottom of magnetic sources and thermal structure of the crust from Cameroon to Central African Republic: Preliminary results for a better understanding of the origin of the Bangui Magnetic Anomaly. *Journal of African Earth Sciences*, 179, 104206. https://doi.org/10.1016/j.jafrearsci.2021.104206.
62. Njiteu, T. C. D., Sobh, M., Basseka, C. A., Mouzong, P. M., Poudjom, D. Y., & Etame, J. (2021b). The mechanical behaviour of the lithosphere beneath the Chad Basin and the Bangui Magnetic Anomaly. Insights from Moho depth and effective elastic thickness estimates. *Journal of African Earth Sciences*, 182, 104299. https://doi.org/10.1016/j.jafrearsci.2021.104299
63. Njiteu, T. C. (2022). The origin of the Bangui Magnetic Anomaly – one of the largest magnetic anomaly in the world. Taylor & Francis, Issue 2016, *Preview of the Australian Society of Exploration Geophysicists*.
64. Nzenti, J. P. (1988). Neoproterozoic alkaline meta-igneous rocks from the Pan-African North Equatorial Fold-Belt (Yaounde, Cameroon): biotite and magnetite rich pyroxenites. *Journal of African Earth Sciences*, 26, 37-47.
65. Okubo, Y., Graft J., Hansen R., Ogawa, K., & Tsu, H. (1985). Curie point depths of the Island of Kyushu and surrounding areas, Japan. *Geophysics*, 53, 481-494. https://doi.org/10.1190/1.1441476
66. Ouabego, K., Quesnel, Y., Rochette, P., Demory, F., Fozing, E. M., Njanko, T., Hippolite, J. C., & Affaton, P. (2013). Rock magnetic investigation of possible sources of the Bangui magnetic anomaly. *Physics of the Earth and Planetary Sciences*. 224, 11-20. https://doi.org/10.1016/j.pepi.2013.09.003
67. Owona, S. (2008). Archean, Eburnean and Pan-African features and relationships in their junction zone in the south of Yaounde (Cameroon). *University of Douala, Unpublished thesis*.
68. Owona, S., Tichomirowa, M., Ratschbacher, L., Mvondo Ondoua, J., Youmen, D., Pfander, J., Tchoua, M. F., Affaton, P., & Ekodeck, E. J. (2012). New igneous zircon Pb/Pb and metamorphic Rb/Sr ages in the Yaounde Group (Cameroon, Central Africa): implications for the Central African fold belt evolution close to the Congo Craton. *International Journal of Earth Sciences*. https://doi.org/10.1007/s00531-012-0751-x
69. Owona, S., Mvondo Ondoua, J., Ekodeck, E. J. (2013). Evidence of Quartz, Feldspar and Amphibole crystal plastic deformations in the Paleoproterozoic Nyong Complex Shear Zones under Amphibole to granulite Conditions (West Central African Fold Belt, Cameroon). *Journal of Geography and Geology*, 5(3). https://doi.org/10.5539/jgg.v5n3p186
70. Penaye, J., Toteu, S. F., Tchameni, R., Van Schmus, W. R., Tchakounte, J., Ganwa, A., Minyem, D., & Nsifa, E. N. (2004). The 2.1 Ga West Central African Belt in Cameroon: *Extension and Evolution*, vol. 39, pp. 159–164.
71. Phillips, J. D. (2000). Locating magnetic contacts: A comparison of the horizontal gradient, analytic signal and local wavenumber methods: 70th Annual International Meeting, SEG, Expanded Abstracts, 402-405.

72. Pin, C., Poidevin, J. L. (1987). U-Pb zircon evidence for a Pan-African granulite facies metamorphism in the Central Africa Republic. A new interpretation of high-grade series of the northern border of the Congo craton. *Precambrian Research*, 36, 303-312.
73. Poidevin, J. (1991). Les ceintures de roches vertes de la république centrafricaine (bandas, boufoyo, bogoin, mbomou). Contribution à la connaissance du précambrien du nord du craton du Congo. *Thèse de doctorat, Université Clermont-Ferrand 2*.
74. Poidevin, J., Dupuy C. (1981). Archean greenstone belt from the Central African Republic (Equatorial Africa). *Precambrian Research*, http://doi.org/10.1016/0301-9268(81)90011-5
75. Poudjom, D. Y., Boukeke D. B., Legeley-Padovani, A., Nnange, J. M., Ateba, B., Albouy, Y., & Fairhead, J. D. (1995). Levés Gravimétriques de reconnaissance, gravity map. *Editions ORSTOM, Institut Français de Recherche Scientifique pour le Developement en Coopération*, 33p.
76. Poudjom Djomani, Y. (1993). Apport de la gravimétrie à l'étude de la lithosphère continentale et implications géodynamiques : étude d'un bombement intra-plaque, le massif de l'Adamaoua (Cameroun). *Thèse de doctorat Ph.D, Université de Paris Sud, Centra Orsay. ORSTOM*, 313p
77. Poudjom Djomani, Y., Diament M., & Albouy Y. (1992). Mechanical behaviour of the lithosphere beneath the Adamawa uplift (Cameroon, West Africa) based on gravity data. *Journal of African Earth Sciences*, 15(1), 81-90.
78. Pratt, D. A., & Zhinqun, S. (2004). An improved pseudo-gravity magnetic transform technique for investigation of deep magnetic source rocks. *ASEG 17th Geophysical conference exhibition, Sidney*.
79. Quintero, W., Enriquez-Campos, O., & Orlando, H. (2019). Curie point depth, thermal gradient, and heat flow in the Colombian Caribbean (northwestern South America). *Geothermal Energy*, 7:16. https://doi.org/10.1186/s40517-019-0132-9
80. Ravat, D. (1989). Magsat Investigations over the Greater African Region. *PhD Thesis University of Purdue*, 253p.
81. Ravat, D., Wang, B., Widermuth, E., & Taylor, P. T. (2002). Gradient in the interpretation of satellite altitude magnetic data an example from Central Africa. *Journal of Geodynamics*, 33, 131-142.
82. Regan, R. D., & Marsh, B. D. (1982). The Bangui Magnetic Anomaly. Its geological origin. *Journal of Geophysical Research*, 87, 1107-1120.
83. Salem, A., Williams, S., Fairhead, D., Smith, R., & Ravat D. (2008). Interpretation of magnetic data using tilt-angle derivatives. *Geophysics*, 73(1), 1-10. https://doi.org/10.1190/1.2799992
84. Shang, C. K., Satir, M., Siebel, W., Nsifa, N. E., Taubald, H., Liegeois, J. P., & Tchoua, F. M. (2004). TTG magmatism in the Congo craton: a view from major and trace element geochemistry, Rb-Sr and Sm-Nd systematics: case of the Sangmelima region, Ntem complex, southern Cameroon. *Journal of African Earth Sciences*, 40, 61-79. https://doi.org/10.1016/j.jafreasci.2004.07.005
85. Shang, C. K., Liegeois, J. P., Satir, M., Frish, W., & Nsifa, E. N. (2010). Late Archean high-K granite geochronology of the northern metacratonic margin of the Archean Congo Craton, Southern Cameroon: evidence for Pb-loss due to non-metamorphic causes. *Gondwana Research*, 18, 337-355. https://doi.org/10.1016/j.gr.2010.02.008

86. Shuey, R., Schellinger, D. K., Tripp A. C., & Alley L. (1976). Curie depth determination from aeromagnetic spectra. *Geophysical Journal of the Royal Astronomical Society*, 50, 75-101.
87. Sobh, M., Ebbing, J., Mansi, A.H., Gotze, H.-J., Emry, E.L., & Abdelsalam, M. (2020). The lithospheric structure of the Saharan metacraton from integrated geophysical and petrological modelling. *Journal of Geophysical Research*, 125, e2019JB018747.
88. Spector, A., & Grant, F. S. (1970). Statistical models for interpretation of aeromagnetic data. *Geophysics*, 35, 293-302. https://doi.org/10.1190/1.1440092
89. Telford, W.M., Geldart, L. P., & Sheriff, R. E. (1990). *Applied Geophysics*. Cambridge University Press, 2nd edition, 760p.
90. Tadjou, J. M., Nouayou, R., Kamguia, J., Houetchack, K. L. & Manguelle-Dicoum, E. (2009). Gravity analysis of the boundary between the Congo craton and the Pan-African belt of Cameroon. *Austrian Journal of Earth Sciences*, 101(2), 71-79.
91. Tanaka, A. (2017). Global Centroid distribution of magnetized layer from world digital magnetic anomaly map. *Tectonics*, 36, 3248-3253. https://doi.org/10.1002/201/2017TC004770
92. Tanaka, A., Okubo, Y., & Maysubayashi, O. (1999). CPD based on spectrum analysis of the magnetic anomaly in East and Southeast Asia. *Tectonophysics*, 306, 461-470.
93. Tessontsap T., Bontognali, T., Ndjigui, P., Vrijmoed, J., Teagle, D., Cooper, M., & Vance D. (2017). Petrography and geochemistry of the Mesoarchean Bikoula iron formation in the Ntem complex (Congo craton), Southern Cameroon: Implication for its origin. *Ore Geology Reviews*, 80, 267-288. https://doi.org/10.1016/j.oregeorev.2016.07.003
94. Thieblemont, D. and partners of the new Africa 10M map project, (2016). An Updated Geological Map of Africa at 1/10000000 Scale. *35th International Geological Congress: IGC 2016, Cape Town, South Africa*.
95. Tokam, K. A., Tabod Tabod, C., Nyblade, A. A., Jordi Julià, Douglas, A. W., & Pasyanos, E. M. (2010). Structure of the crust beneath Cameroon, West Africa, from the joint inversion of Rayleigh wave group velocities and receiver functions. *Geophysical Journal International*, https://doi/org/10.1111/j.1365-246X.201004776
96. Toteu, S. F., Maarten de W., Penaye, J., Kerstin, D., Tait, J. A., Houketchang, M., Van Schmus, W. R., Hielke, J., Moloto-A-Kenguemba, G., Adejardo, F., Lerouge C., & Moctar D. (2022). Geochronology and correlations in the Central African fold belt along the northern edge of the Congo Craton: New insights from U-Pb dating of zircons from Cameroon, Central African Republic and south-western Chad. *Gondwana Research*, 107, 296-324. https://doi.org/10.1016/j.gr.2022.03.010
97. Toteu, S. F. Penaye, J., Deloule, E., Van Smuchs, W. R., & Tchameni, R. (2006). Diachronous evolution of volcano-sedimentary basins north of the Congo craton: insights from U-Pb ion microprobe dating of zircons from the Poli, Lom and Yaounde groups (Cameroon). *Journal of African Earth Sciences*, 44, 428-442. https://doi.org/10.1016/j.jafrearsci.2005.11.011
98. Toteu, S. F., Penaye, J., & Poudjom Djomani, Y. (2004). Geodynamic evolution of the Pan-African belt in central Africa with special reference to Cameroon. *Canadian Journal of Earth Sciences*, 41, 73-85.

https://doi.org/10.1139/E03-079

99. Vervelidou, F., & Thebault, E. (2015). Global map of the magnetic thickness and magnetization of the Earth's lithosphere. *Earth, Planets and Space*, 67, https://doi.org/10.1186/s40623-015-0329-5

100. Zhang, Q., Zhang, Y.T., Yin G., & Li, N. Z. (2018). An improved frequency-domain algorithm for stable reduction to the pole at low latitudes. *Journal of Geophysics and Engineering*, 15, 1767–1782. https://doi.org/10.1088/1742-2140/aaa227

Figures

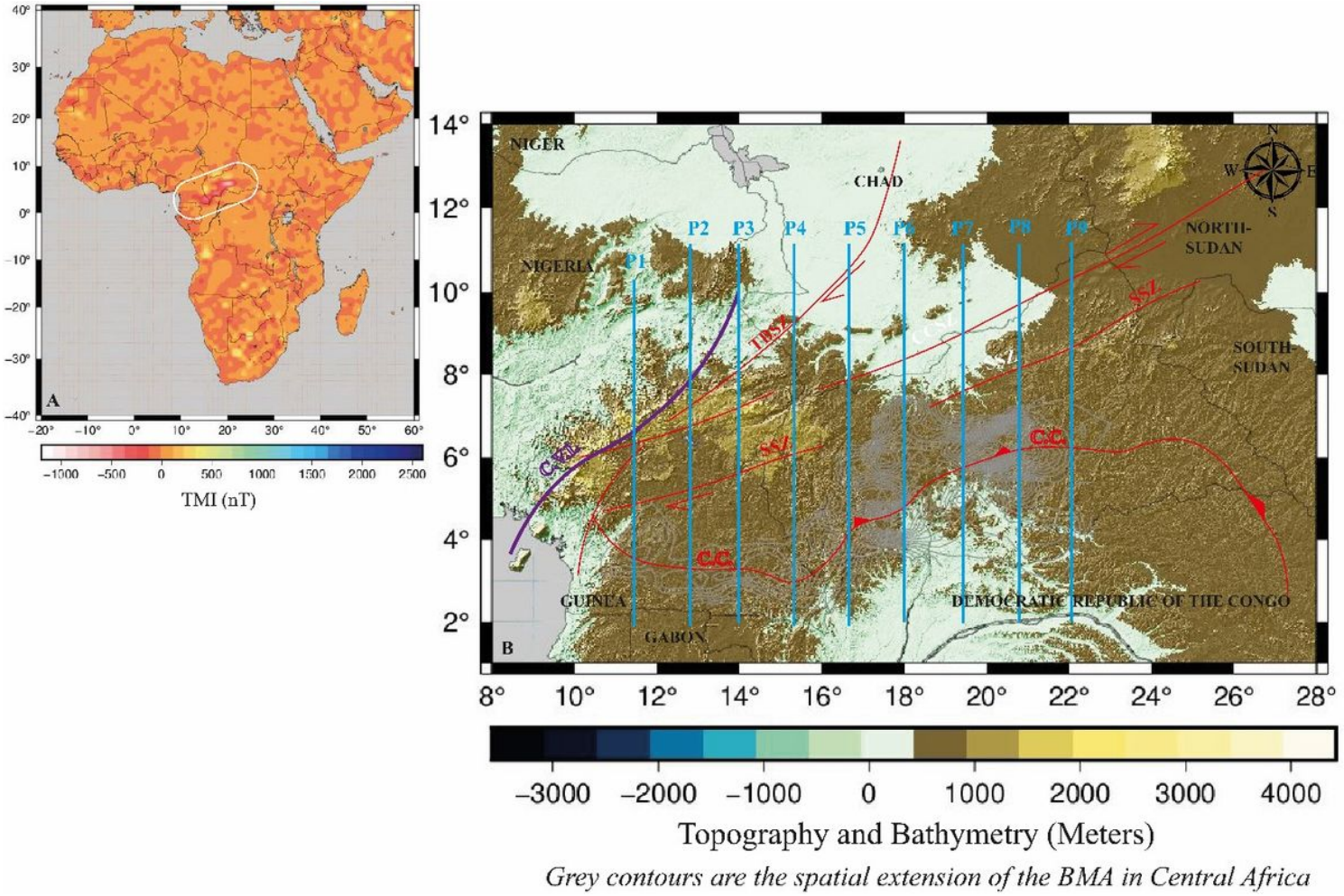

Figure 1

Location of the study area. (A) An overview of the BMA in Central Africa (in white circle), derived from the EMAG2-v3 magnetic data (Meyer et al., 2017); (B) Topography map of Central Africa overlayed by the main lithospheric structures, showing the spatial extension of the BMA in the continental part (Cameroon and Central African Republic). TBSZ-Tchollire-Banyo Shear Zone; CCSZ-Central Cameroon Shear Zone; SSZ-Sanaga Shear Zone; CVL-Cameroon Volcanic Line. P1 – P9 are the location of the two-dimensional gravity and magnetic models.

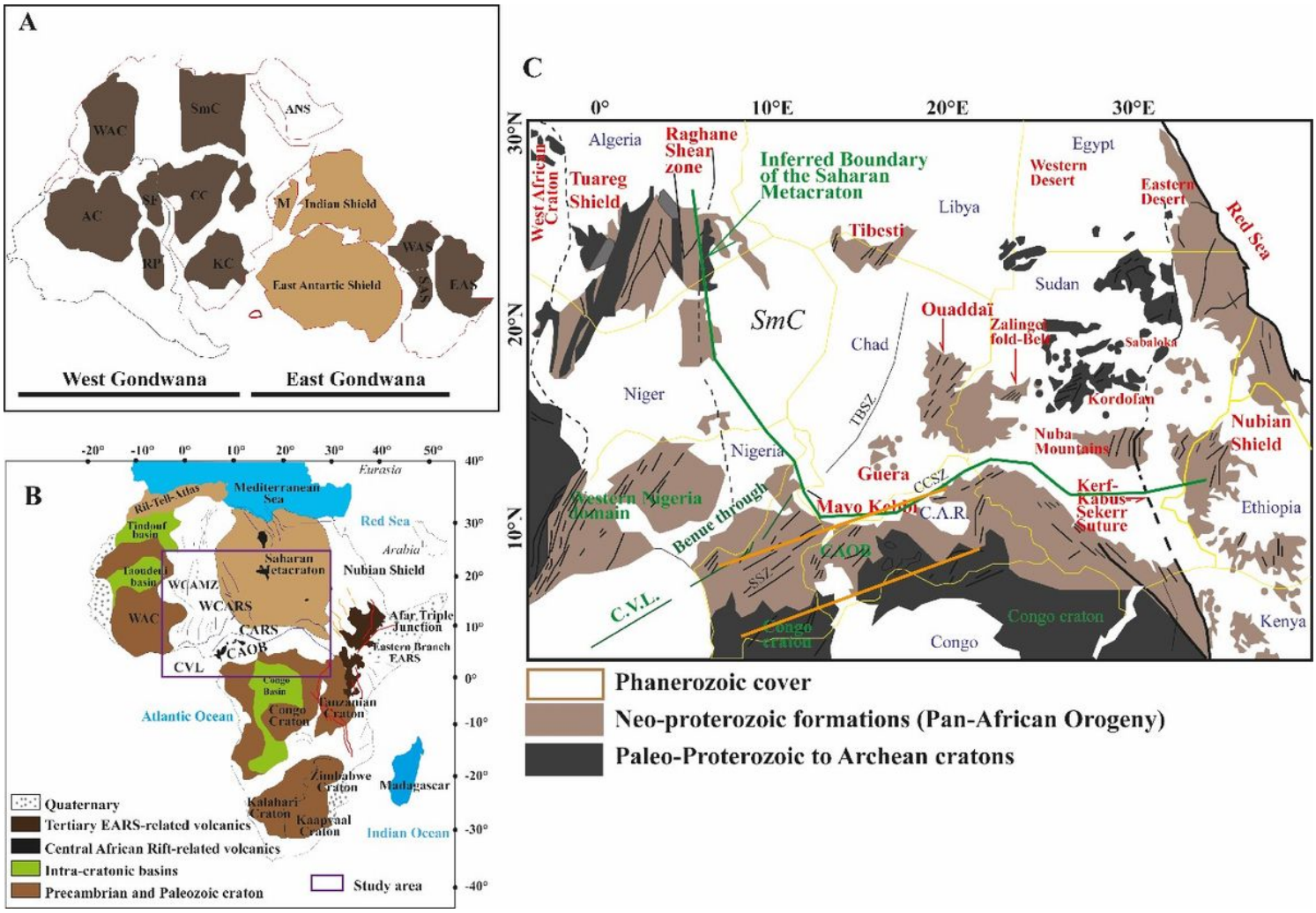

Figure 2

(A) regional setting in Gondwana tectonic plates and the Neoproterozoic belts (after Gray et al., 2007), WAC- West African Craton, AC-Amazonian Craton, SmC-Saharan Metacraton, CC-Congo Craton, KC-Kalahari Craton, ANS-Arabian Shield, WAS-West Antarctic Shield, EAS-East Antarctic Shield, SAS-South Antarctic Shield, M-Mozambique Belt, San Francisco Craton, RP-Rio Plata Craton; - (B) Location of the study area on a simplified tectonic map of Africa (after Milesi et al., 2010). Also shown are the Archean cratons, intracratonic basins and the surrounding Precambrian and Paleozoic fold belts, affected by rifting processes during Mesozoic and Cenozoic times and Cenozoic volcanism. WCAMZ: West and Central African Mobile Zone, WCARS: West and Central African Rift System, CVL-Cameroon volcanic line, EAR-East African Rift, WAC-West African Craton; - (C) Simplified geological map showing the Central African Orogenic Belt in the West and Central African Rift System and the Congo Craton (modified after Abdelsalam et al., 2002). TBSZ-Tchollire-Banyo Shear Zone; CCSZ-Central Cameroon Shear Zone; C.V.L.-Cameroon Volcanic Line, SmC-Saharan Metacraton, C.A.R-Central African Republic. Orange lines outline the location of the BMA.

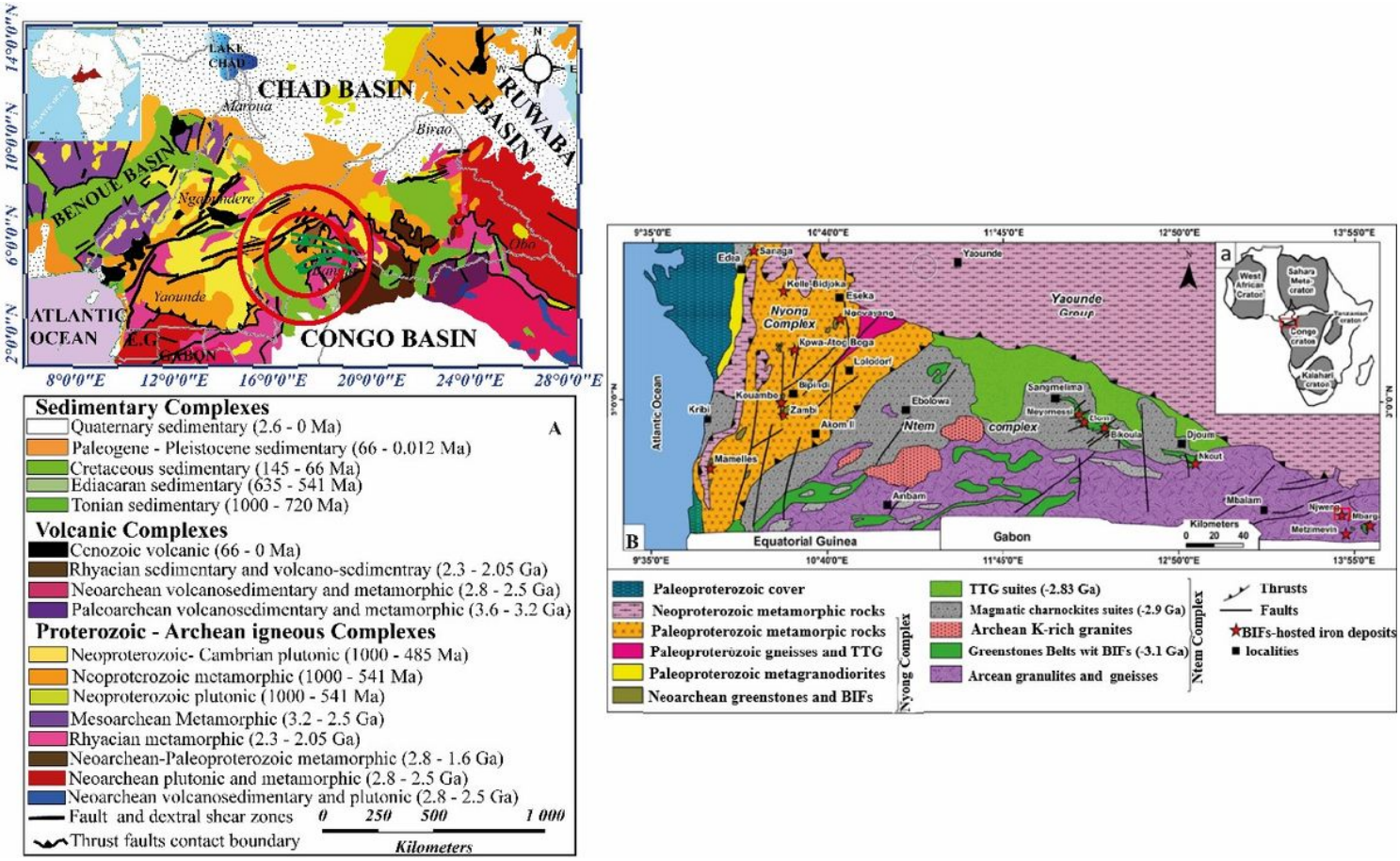

Figure 3

(A) Simplified geological map of Cameroon, Central African Republic and adjacent countries, modified from the International Geological Map of Africa (Thieblemont et al., 2016) overlain by greenstone belts (green lines) of Banda – Boufoyo and Bogoin (after Ki-Kis et al., 2021; Dostal et al., 1985). The red circles indicate the position of the impact structure described by Girdler et al. (1992). (B) Geological map of the southern Cameroon showing the locations of the BIFs and greenstones belts.

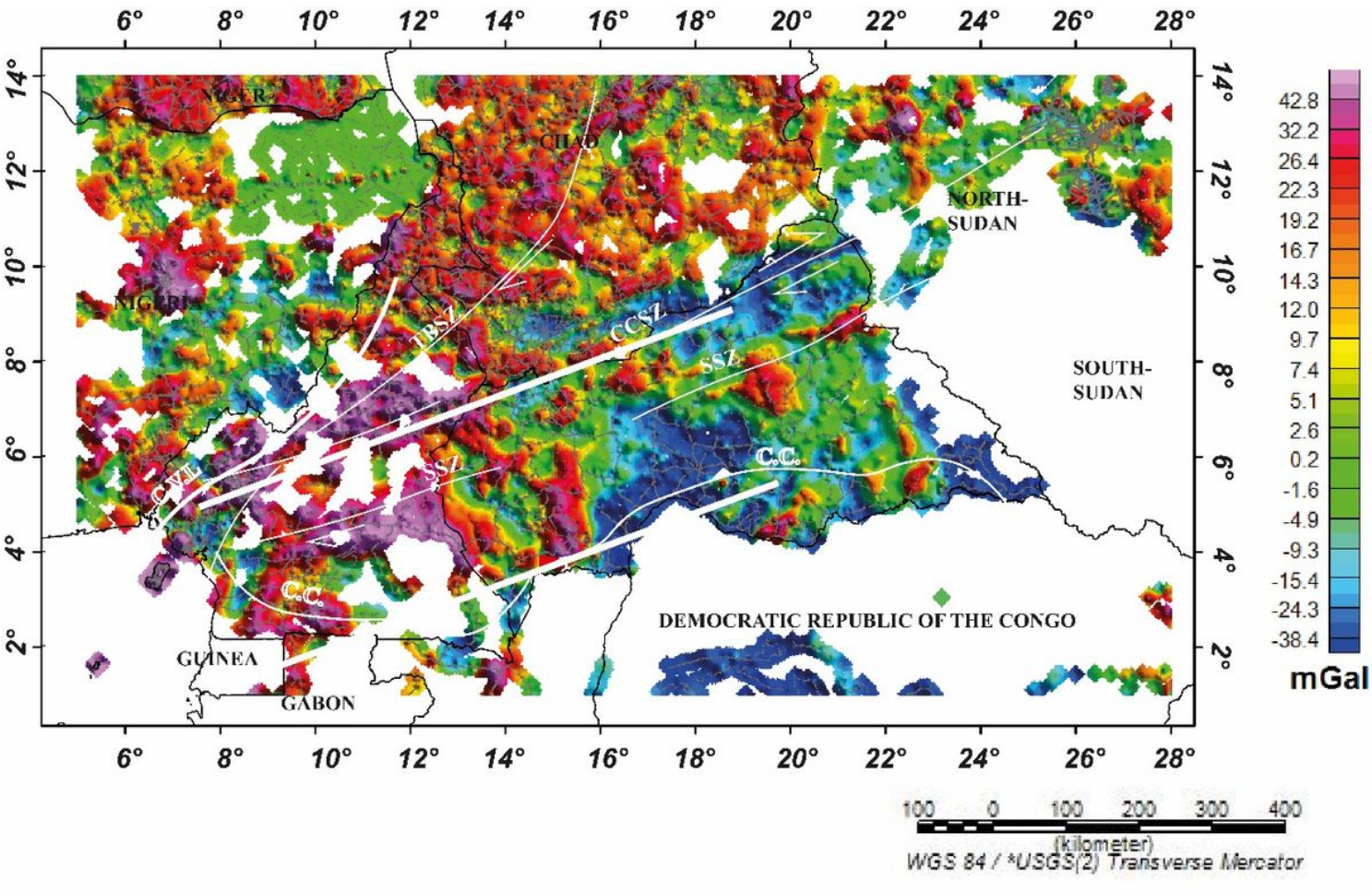

Figure 4

Free air gravity anomaly map in Central Africa showing the spatial correlation with the BMA. Solid blue lines (P1 – P9) are the profiles used for the forward modelling. The White thick lines represent the boundary of the BMA; CVL: Cameroon Volcanic Line; CCSZ: Central Cameroon Shear Zone; SSZ: Sanaga Shear Zone; TBSZ: Tchollire Banyo Shear Zone. Grey points on the map are the gravity stations.

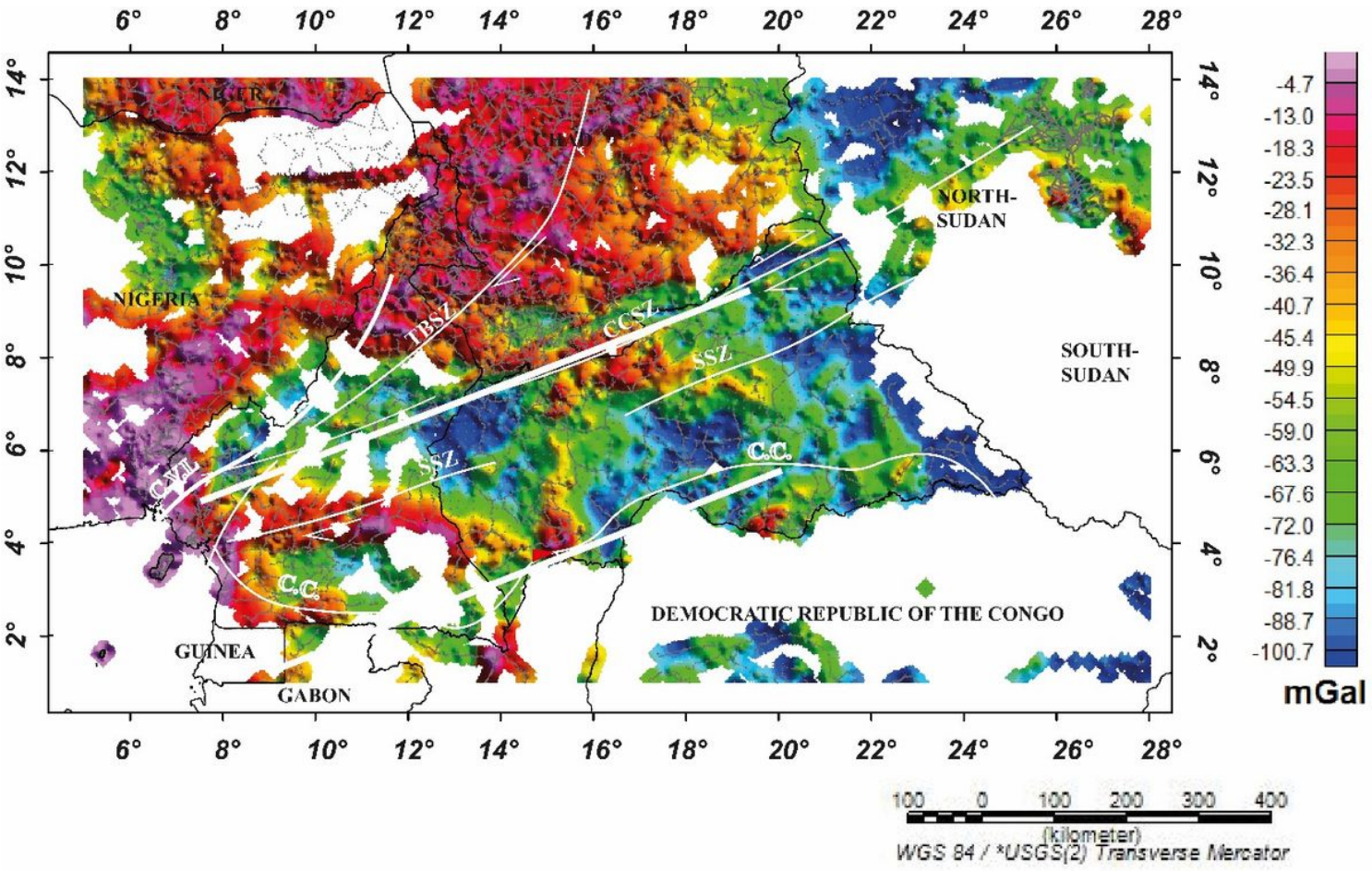

Figure 5

Complete Bouguer gravity anomaly map in Central Africa showing the spatial correlation with the BMA. Solid blue lines (P1 – P9) are the profiles used for the forward modelling. The White thick lines represent the boundary of the BMA; CVL: Cameroon Volcanic Line; CCSZ: Central Cameroon Shear Zone; SSZ: Sanaga Shear Zone; TBSZ: Tchollire Banyo Shear Zone.

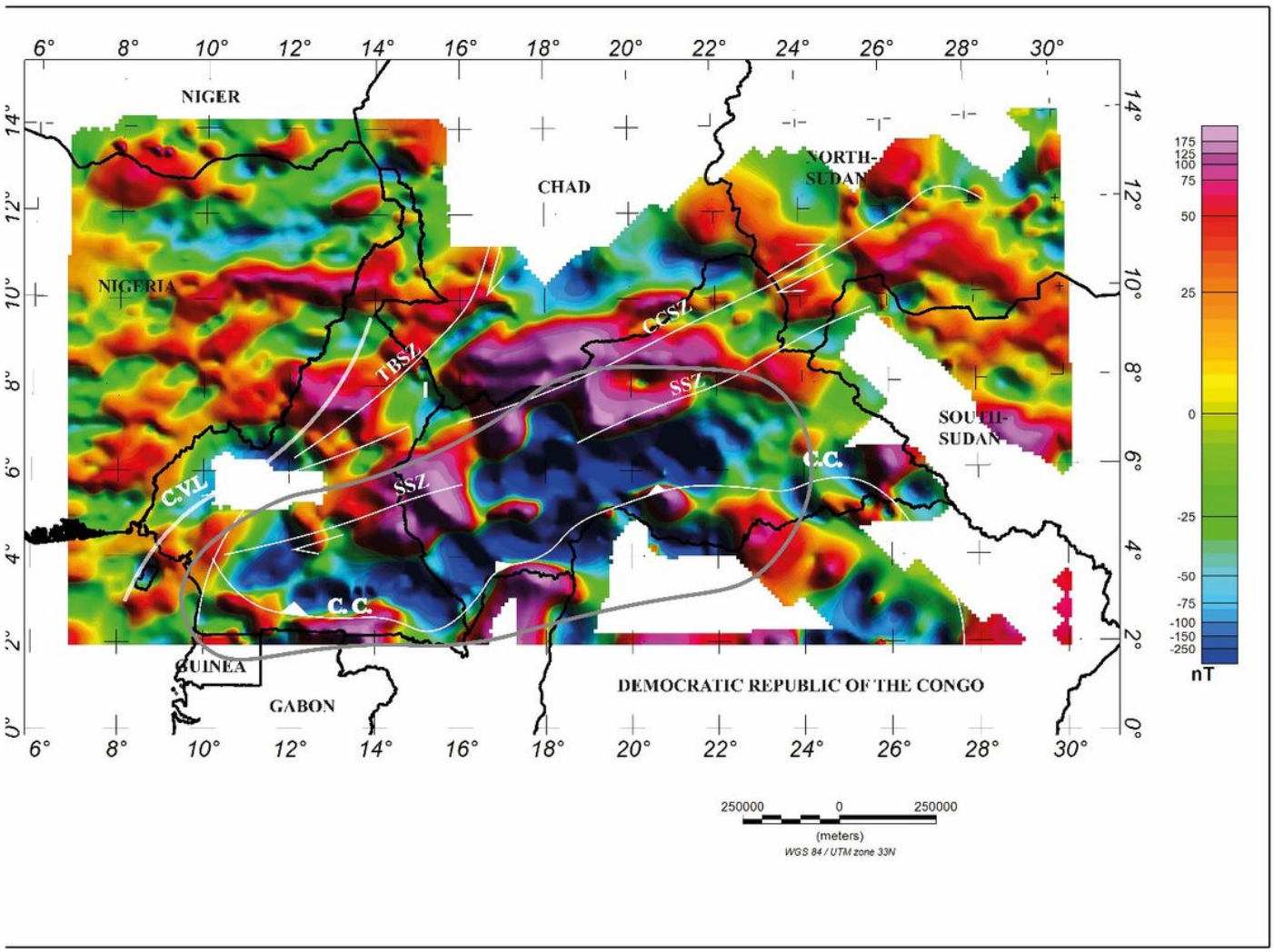

Figure 6

Total magnetic intensity map derived from the EMAG2-v3 model. the grey contour line represents where of the BMA is associated with shear zones. CVL: Cameroon Volcanic Line; CCSZ: Central Cameroon Shear Zone; SSZ: Sanaga Shear Zone; TBSZ: Tchollire Banyo Shear Zone.

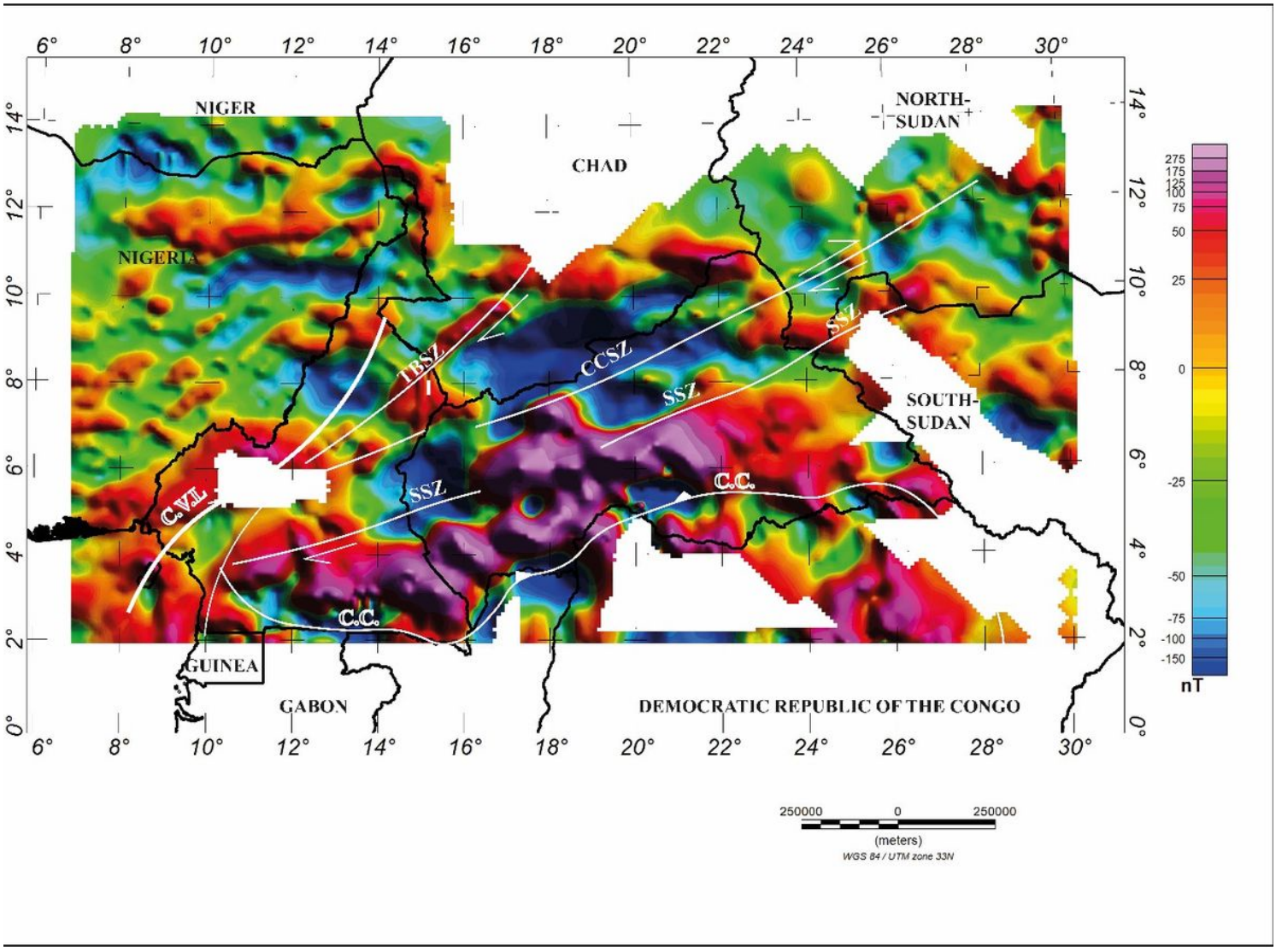

Figure 7

Total magnetic intensity map reduced to the pole, showing the location of the selected profiles (P1 to P9) used for the gravity and magnetic forward modelling across the BMA. CVL: Cameroon Volcanic Line; CCSZ: Central Cameroon Shear Zone; SSZ: Sanaga Shear Zone; TBSZ: Tchollire Banyo Shear Zone; C.C.: Congo Craton

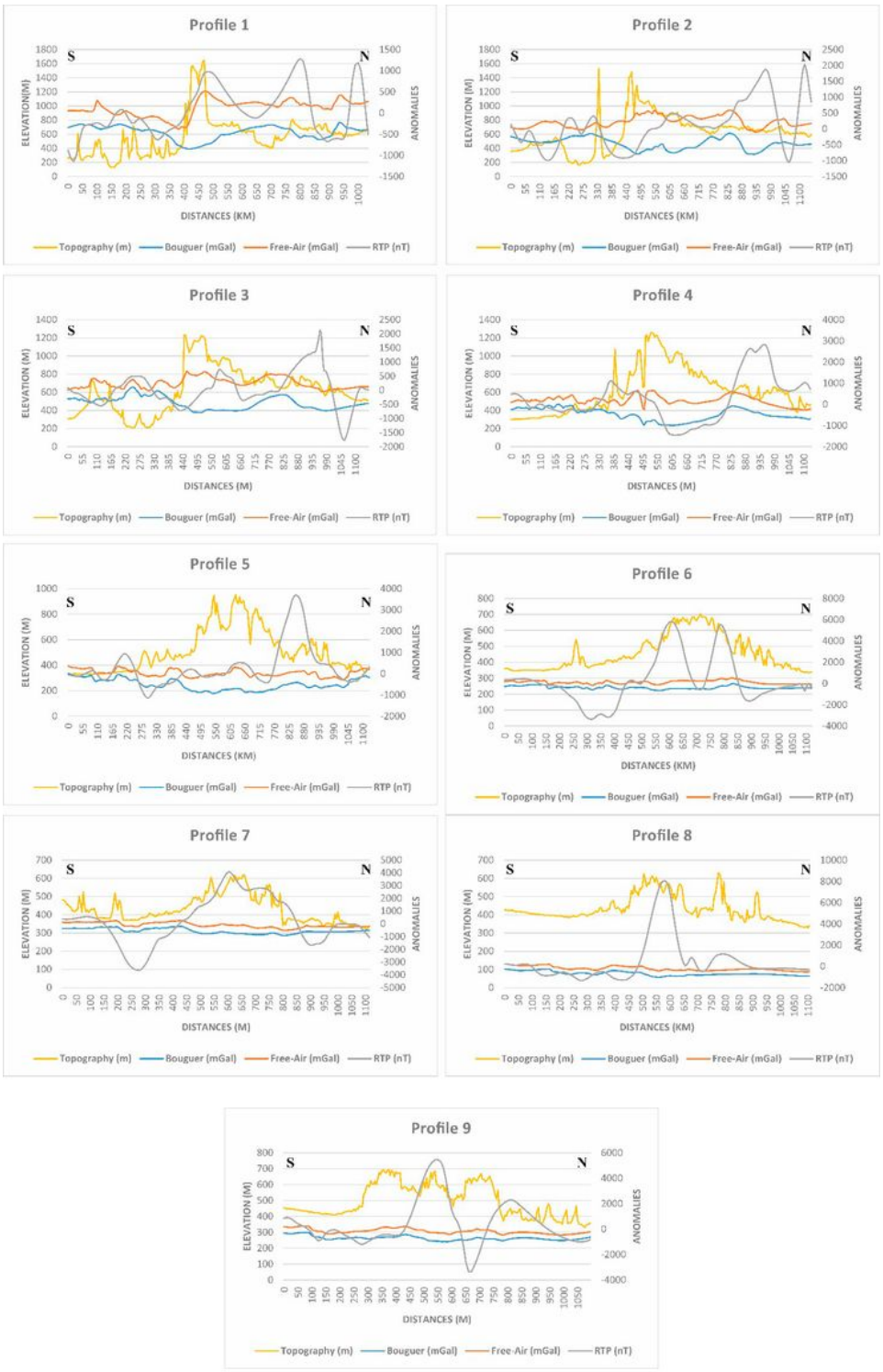

Figure 8

Plots of the P1 - P9 (Fig. 1) showing the topography, Free-air gravity, complete Bouguer gravity anomalies and the RTP magnetic anomalies

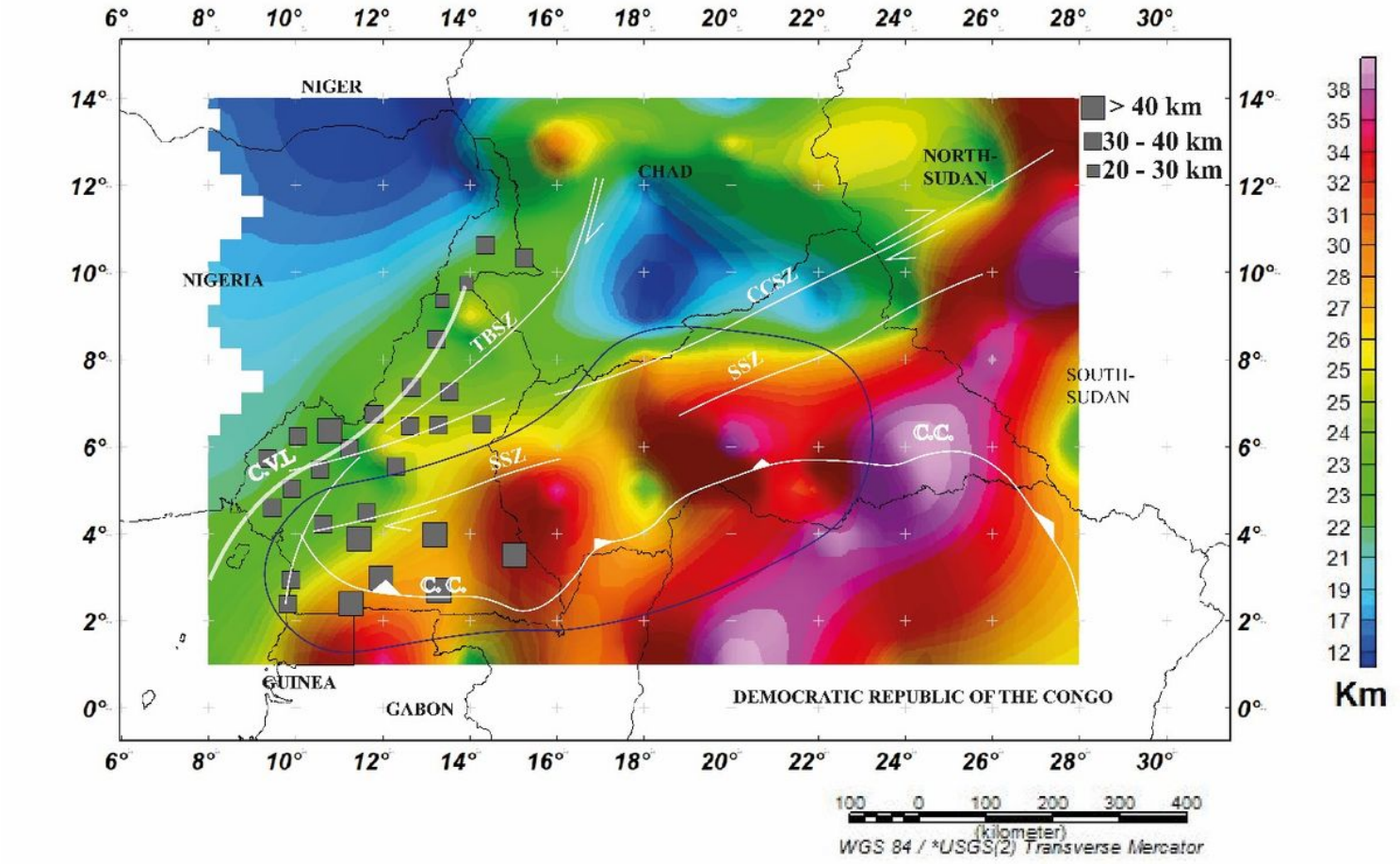

Figure 9

Curie isothermal depths beneath the BMA (1) area express by the blue circle in Central Africa (modified after Njiteu et al. 2021a). CVL: Cameroon Volcanic Line; CCSZ: Central Cameroon Shear Zone; SSZ: Sanaga Shear Zone; TBSZ: Tchollire Banyo Shear Zone. Grey squares are the depths to the crust-mantle boundary found from broadband seismic studies (Tokam et al., 2010; Gallacher and Bastow, 2012)

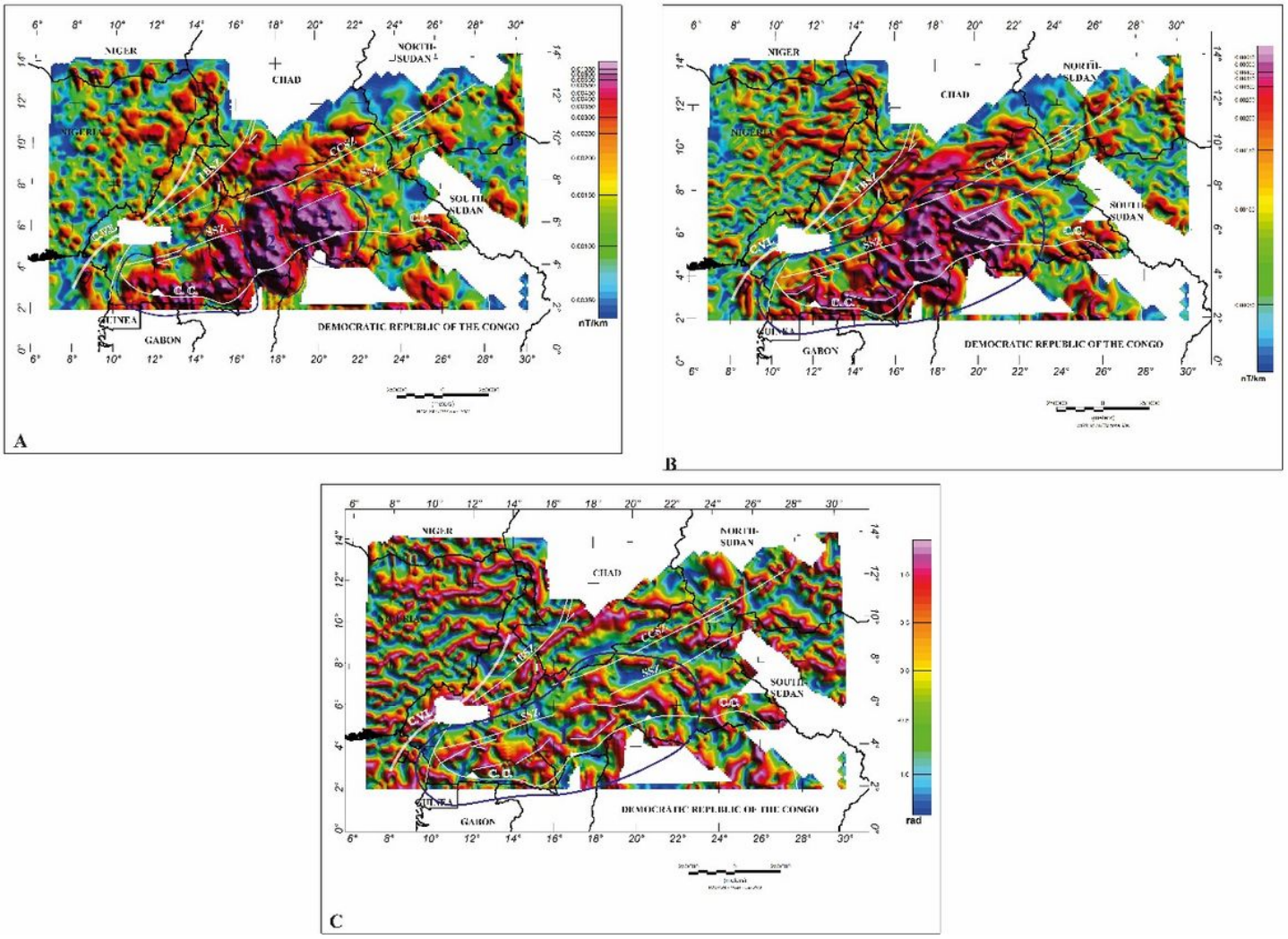

Figure 10

(A) Analytic signal of the RTP magnetic data. The blue contours traduce a localised sources beneath the BMA: (1) localised circular anomaly; (2) N-S anomaly with an E-W secondary anomalies; (3) E-W anomaly along the northern edge of the Congo Craton in Cameroon. (B) Horizontal derivative of the RTP data. The blue circle expressed the spatial extension of the BMA with the E-W secondary gradient (1). (C) Tilt-derivative of the RTP magnetic data showing the E-W direction of the secondary gradient zones along the BMA (1) expressed by the blue circle. CVL: Cameroon Volcanic Line; CCSZ: Central Cameroon Shear Zone; SSZ: Sanaga Shear Zone; TBSZ: Tchollire Banyo Shear Zone.

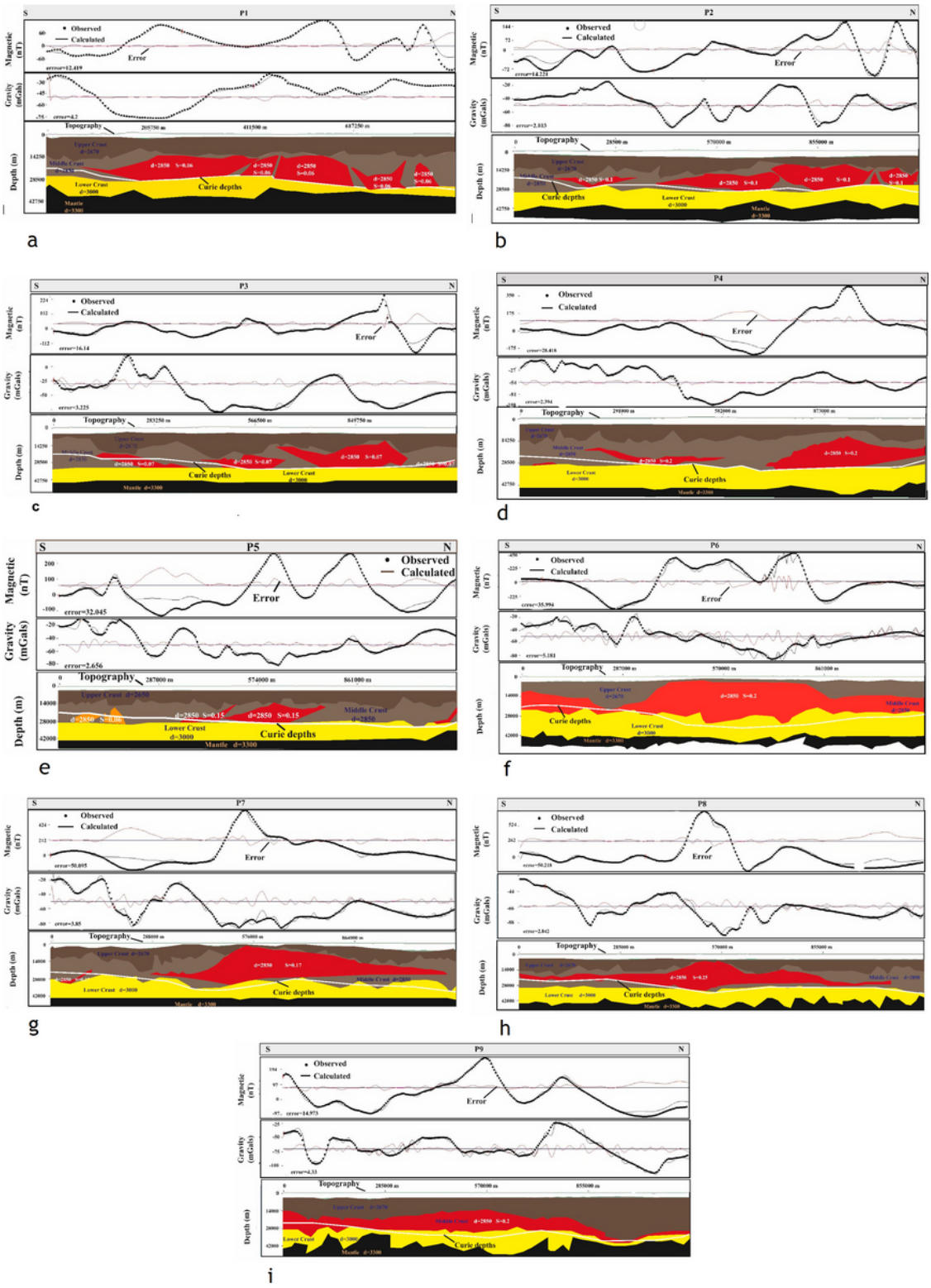

Figure 11

11a. Two-dimensional gravity and magnetic forward model (P1, Figs. 5 and 7) across the BMA. d is density in kg/m^3 and S is magnetic susceptibility in SI units.

11b. Two-dimensional gravity and magnetic forward model (P2, Figs. 5 and 7) across the BMA. d is density in kg/m^3 and S is magnetic susceptibility in SI units

11c**.** Two-dimensional gravity and magnetic forward model (P3, Figs. 5 and 7) across the BMA. d is density in kg/m^3 and “S” is magnetic susceptibility in SI units.

11d. Two-dimensional gravity and magnetic forward model (P4, Figs. 5 and 7) across the BMA. d is density in kg/m^3 and “S” is magnetic susceptibility in SI units.

11e. Two-dimensional gravity and magnetic forward model (P5, Figs. 5 and 7) across the BMA. d is density in kg/m^3 and S is magnetic susceptibility in SI units.

11f. Two-dimensional gravity and magnetic forward model (P6, Figs. 5 and 7) across the BMA. d is density in kg/m^3 and S is magnetic susceptibility in SI units

11g. Two-dimensional gravity and magnetic forward model (P7, Figs. 5 and 7) across the BMA. d is density in kg/m^3 and S is magnetic susceptibility in SI units.

11h. Two-dimensional gravity and magnetic forward model (P8, Figs. 5 and 7) across the BMA. d is density in kg/m^3 and S is magnetic susceptibility in SI units.

11i. Two-dimensional gravity and magnetic forward model (P9, Figs. 5 and 7) across the BMA. d is density in kg/m^3 and S is magnetic susceptibility in SI units.